Multiple losses of ecdysone receptor genes in nematodes: an alternative evolutionary scenario of molting regulation

Shumpei Yamakawa[1*], Lisa-Marie Barf[1], and Andreas Hejnol[1,2*]

1. Institute of Zoology and Evolutionary Research, Faculty of Biological Sciences, Friedrich Schiller University Jena, Jena, Germany

2. Department of Biological Sciences, University of Bergen, Bergen, Norway

*Corresponding authors: Andreas Hejnol, Shumpei Yamakawa

Email: andreas.hejnol@uni-jena.de, shumpei.yamakawa@gmail.com

ORCID: S.Y.: 0000-0002-2557-0670, L.-M.B: 0000-0001-7535-2690, A.H.: 0000-0003-2196-8507

Author Contributions: Conceptualization, S.Y..; methodology, S.Y. and L.-M.B.; software, S.Y. and L.-M.B.; formal analysis, S.Y.; investigation, S.Y and L.-M.B..; writing—original draft, S.Y.; writing—review & editing, S.Y., L.-M.B., and A.H.; visualization, S.Y.; funding acquisition, S.Y. and A.H.

Competing Interest Statement: The authors declare no competing interests.

Keywords: nematodes, ecdysone, molting, *ecr*, *nhr-23/hr3*.

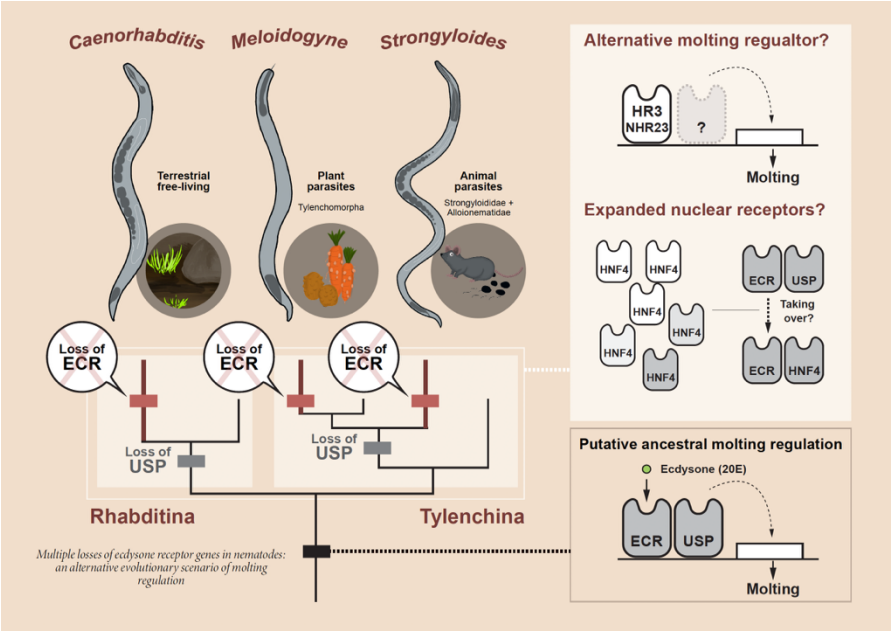

Abstract

Molting is a hallmark feature of ecdysozoans, including arthropods, tardigrades, and nematodes. Ecdysone hormones play a crucial role in regulating the molting process of different ecdysozoan taxa. Interestingly, despite this highly conserved function of ecdysone, the model nematode *Caenorhabditis elegans* has lost the ecdysone receptor (ECR) genes and their molting appears to be ecdysone-independent. The loss of *ecr* has only been reported in *Caenorhabditis* within ecdysozoans, and the evolutionary background behind this loss has remained enigmatic. Here, we show that loss of *ecr* is not exceptional in *Caenorhabditis*, but has occurred at least three times in Rhabditina and Tylenchina nematodes. Our genome-wide analysis of 160 nematode species revealed multiple losses of *ecr* and its typical heterodimer partner *usp* during nematode evolution. Furthermore, using transcriptomic and *in silico* protein structural analyses, we identified two factors that potentially underlie and buffer the loss of ECR gene/function: (1) molting regulation by an alternative nuclear receptor HR3 (NHR-23) and (2) a lineage-specific expansion of nuclear receptors in the *ecr*-deficient taxa. Taken together, this study shows how key regulators of ecdysozoan molting can be altered during evolutionary process. We propose a novel scenario for the evolution of molting regulation, highlighting the importance of HR3 as the potential core regulator.

Introduction

Ecdysozoa, which includes arthropods, nematodes, priapulids, and others, comprises more than 80% of all animal species (Aguinaldo, et al. 1997; Dunn, et al. 2008; Hejnol, et al. 2009). A defining feature of ecdysozoans is their ability to grow and change appearance by periodically shedding a cuticular exoskeleton (Nielsen 2012; Giribet and Edgecombe 2017; Schumann, et al. 2018). As the name Ecdysozoa derives from this unique growth strategy, molting or ecdysis (Aguinaldo, et al. 1997), the acquisition of a cuticular exoskeleton and molting process is a key innovation in ecdysozoan evolution. Despite its importance for understanding of ecdysozoan evolution, the evolutionary background of molting remains enigmatic.

Molting regulation has been well characterized in arthropods such as insects and decapods, and ecdysone hormone is a master regulator governing molting in arthropods (Fig. 1B) (Lachaise, et al. 1993; Thummel 1996; Yamanaka, et al. 2013; Niwa and Niwa 2014; Hyde, et al. 2019). For example, ecdysone hormone is synthesized from cholesterol by a group of genes called the Halloween genes (e.g., *sad* and *phm*) in specific endocrine organs such as the prothoracic glands. The secreted ecdysone is converted to 20-hydroxyecdysone (20E), which binds to the ecdysone receptor (ECR) in the target tissues (e.g., epidermal cells). The ecdysone receptor (ECR) forms a heterodimer with another nuclear receptor USP to activate downstream cascade genes (e.g., HR3 and FTZ-F1, Fig. 1B). Ecdysone signaling is also known to be involved in various developmental and physiological processes such as reproduction (Kozlova and Thummel 2000; Subramoniam 2000). Recently, we also found that tardigrade molting is likely regulated by ecdysteroid hormone (Yamakawa and Hejnol 2024), suggesting that ecdysone-dependent molting is ancestral in panarthropods.

Ecdysone hormone also potentially regulates the molting of nematodes (Barker and Rees 1990; Barker, et al. 1990). Particularly, the involvment of ecdysone in molting has been suggested in Spirurina nematodes. For example, endogenous ecdysteroids have been detected in various Spirurina species, including *Anisakis simplex*, *Dirofilaria immitis*, and *Ascaris suum* (Fleming 1985; Cleator, et al. 1987; Evershed, et al. 1987). In *Ascaris suum*, 20E exhibits pulsatile fluctuations synchronized with the molting cycle, resembling patterns reported in arthropods (Fleming 1985). The functions of ecdysone have also been tested using pharmacological analysis; the treatment of exogenous 20E or RH5849 (an ecdysone agonist) stimulates molting or larval growth in *Ascaris suum* (L2-L3) and *Dirofilaria immitis* (L3-L4 and microfilarial development) (Fleming 1985; Barker, et al. 1990; Barker 1992; Shang Kuan and Prichard 2020). The functionality of ECR-USP heterodimer has been also shown in *Brugia malayi* (Tzertzinis, et al. 2010). Morover, a pleiotropic function of ecdysone is also suggested in nematodes, as ecdysone may regulate oocyte development in *D. immitis* and microfilarial release in *Brugia pahangi* (Delves, et al. 1986; Barker, et al. 1991). Even outside of Spirurina, the detection of ecdysone and the induction of molting by exogenous ecdysone have been reported in Trichinellida and Rhabditina nematodes (Hitcho and Thorson 1971; Dennis 1976; Barker and Rees 1990; Barker, et al. 1990; Graham, et al. 2010). The above reports support a pivotal role of ecdysone in molting and development of nematodes and hence ecdysozoans.

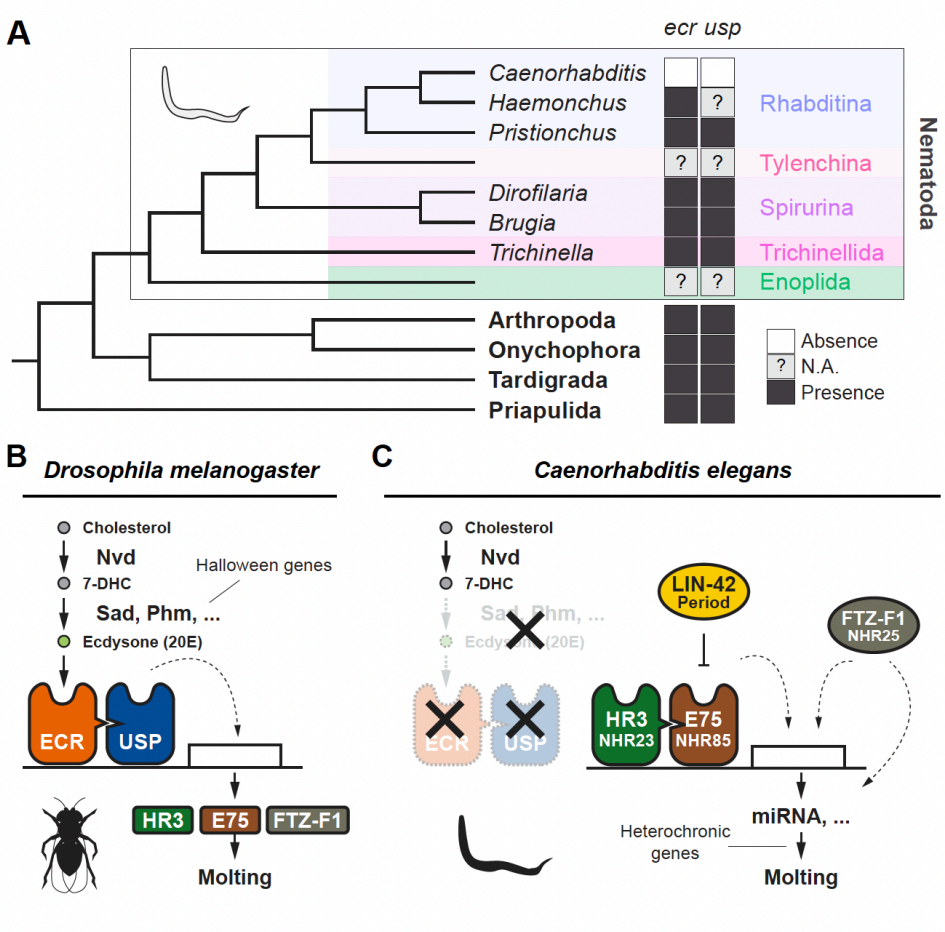

Figure 1. Presence of ecdysone receptors and molting regulation in ecdysozoans
A: Presence and absence of the ecdysone receptor (*ecr*) and its heterodimer partner gene *usp* in ecdysozoan taxa (Shea, et al. 2004; Bonneton, et al. 2008; Graham, et al. 2010; Parihar, et al. 2010; Shea, et al. 2010; Tzertzinis, et al. 2010; Schumann, et al. 2018). As shown in the legends of the panels, black, gray, and white indicate the presence, no information (N.A.), and absence of the genes, respectively. **B** and **C**: Schematic diagrams of the molting regulatory mechanisms in *Drosophila melanogaster* and *Caenorhabditis elegans*, respectively. 20E (20-hydroxyecdysone) is synthesized from cholesterol by the Nvd and Halloween genes, such as Sad (Shadow) and Phm (Phantom). The ECR-USP heterodimer binds to 20E, activating a cascade of downstream genes, including HR3, E75, and FTZ-F1. *C. elegans* is known to lack genes that synthesize ecdysone and its receptors, which play an important regulatory role in insect molting. See the main text for details on each regulatory mechanism.

Interestingly, however, the model nematode *Caenorhabditis elegans* is known to lack any genes coding the ecdysone hormone receptor (ECR) (Schumann, et al. 2018; Taubenheim, et al. 2021). As *ecr* has been identified in different nematode taxa (Shea, et al. 2004; Graham, et al. 2010; Parihar, et al. 2010; Shea, et al. 2010; Tzertzinis, et al. 2010), loss of *ecr* in *C. elengas* is so far the only demonstrated case among ecdysozoans (Fig. 1A). *C. elegans* is also known to lack any genes coding *usp* (Schumann, et al. 2018; Taubenheim, et al. 2021), and molting of *C. elegans* must be therefore independent of

ecdysone (Frand, et al. 2005; Hill, et al. 2013). Rather, the molting of *C. elegans* is regulated by a mechanism similar to the biological/circadian clock (Fig. 1C) (Hendriks, et al. 2014; Meeuse, et al. 2020; Tsiairis and Großhans 2021; Meeuse, et al. 2023). For example, evolutionary conserved components of circadian clock, HR3/NHR-23 (ROR), LIN-42 (Period), and E75/NHR-85 (Rev-Erb), dominantly regulate the molting periods in *C. elegans* (Kostrouchova, et al. 1998, 2001; Frand, et al. 2005; Kouns, et al. 2011; Monsalve, et al. 2011; Patel, et al. 2022; Johnson, et al. 2023; Kinney, et al. 2023; Hiroki and Yoshitane 2024; Spangler, et al. 2024). Kinney et al. 2023 proposed a model of the molting clock in *C. elegans*; the temporal formation of HR3/NHR-23 and E75/NHR-85 heterodimer generates a transcriptional pulse of the microRNA *lin-4*, and LIN-42 is also involved in this process by suppressing E75/NHR-85 expression (Fig. 1C) (Kinney, et al. 2023). Feedback loops involving HR3/NHR-23 and other genes/microRNAs (e.g., *let-7*) have also been identified in *C. elegans* (Kouns, et al. 2011; Patel, et al. 2022; Johnson, et al. 2023). Interestingly, NHR-25, an ortholog of FTZ-F1 which regualtes insect molting, is a core regualtor of *C. elegans* molting (Fig. 1B, C) (Gissendanner, et al. 2004; Hayes, et al. 2006; Hada, et al. 2010).

Ecdysone-independent molting in *C. elagans* is considered as a derived state within nematodes. The loss of *ecr in C. elegans* also seems to contradict the conserved stereotypic molting in nematodes, in which most species consistently molt four times regardless of the divergence in the life cycles (Malakhov 1986). Thus, it is generally considered that the loss of *ecr* in *C. elegans* is an extremely specific and rare event (Taubenheim, et al. 2021), and elucidating the evolutionary background of *ecr* loss has been a long-standing challenge. The loss of *ecr* in *C. elegans* is a critical subject for understanding the evolution of ecdysozoan molting since it is implied that a key regulator of molting can be altered during evolutionary process. Shortly, the case of *C. elegans* raises doubts on the evolutionary conserved role of ecdysone.

This study investigated the evolutionary trajectory leading to the loss of *ecr* and *usp* in nematodes, aiming to elucidate how key regulators of ecdysozoan molting can be altered. We examined the presence of *ecr* and *usp* in a total of 160 nematode species and elucidated the evolution of nematode molting regulation using genomic, transcriptomic, and *in silico* protein prediction analyses.

Results

1. Multiple losses of *ecr* and *usp* genes in Rhabditina and Tylenchina nematodes

Although *ecr* genes have been identified in some nematodes outside *Caenorhabditis* (Fig. 1A) (Shea, et al. 2004; Graham, et al. 2010; Parihar, et al. 2010; Shea, et al. 2010; Tzertzinis, et al. 2010), the specificity of *ecr* loss has been insufficiently explored within a phylogenetic framework. Thus, using publicly available genomic and transcriptome data, we searched for *ecr* across 160 nematode species including major nematode taxa (Fig. 2A, B, 159 genomic and 1 transcriptomic data, see also the methods). The genes of *ecr* were searched using BLAST and phylogenetic analysis (see the methods).

Gene mining of ecr and usp in 160 nematode species

Our search identified *ecr* genes from all major nematode taxa, including the sister group of all remaining nematodes, Enoplida (Fig. 2A). In Rhabditina, *ecr* was absent, not only in *C. elegans*, but in all *Caenorhabditis* species examined (Fig. 2A). Considering that *ecr* is present in other Rhabditina species (Fig. 2A), the loss of *ecr* is specific to the *Caenorhabditis* lineage. Unexpectedly, *ecr* is also absent in 26 of 41 Tylenchina species examined (Fig. 2A). Based on the currently supported phylogeny (see methods) (Smythe, et al. 2019; Ahmed, et al. 2022; Qing, et al. 2024), the loss of *ecr* is indicated as occurring twice in Tylenchina (Fig. 2A, C). Together, the loss of *ecr* occurred at least three times during nematode evolution. Note that the *ecr* genes, previously identified in *Strongyloides* species (Gonzalez Akimori, et al. 2021*)*, are incorrectly annotated (Fig. S1).

C. elegans is also known to lack the gene encoding USP (Taubenheim, et al. 2021), a typical heterodimer partner of ECR. Our gene mining revealed that *usp* is also absent in several lineages of Rhabditina and Tylenchina (Fig. 2A). Especially, the loss of *usp* is detected not only in the species lacking *ecr* but more broadly observed as no *usp* was identified in some Rhabditina species having *ecr* (ex., Strongylida: Fig. 2A, C). The loss of *usp* also precedes the loss of *ecr* in Tylenchina as only Steinernematidae have both *ecr* and *usp* (Fig. 2A, C). The correlation of the loss of *ecr* and *usp* suggests that the ECR-USP functionality has been lost several times in nematodes. It should also be noted that there are no correlation of *ecr* and *usp* losses with specific lifestyle/habitat (Fig. 2A).

Additional analyses of ecr and usp loss

We confirmed that the absence of *ecr* and *usp* is not due to technical errors or low-quality genome assembly (Figs S2–S4, genome size, number of scaffolds, assembly N50, and BUSCO score). As these figures show, no correlation with specific metrics was observed. We also surveyed ecdysone receptors (*ecr* and *usp*) and biogenetic genes (Halloween genes, Fig. 1B) in ecdysozoans and nematodes, respectively, motivated by our unexpected finding of multiple *ecr* losses. We obtained consistent results with previous reports. For example, *ecr* was newly identified in all ecdysozoan species examined (Fig. S5): nematomorphs (Gordioida and Nectonematoida), tardigrades (Heterotardigrada),

kinorhynchs, and priapulids. No Halloween genes (*spo*, *phm*, *dib*, *sad*, or *shade*) were identified in any of the nematode species examined.

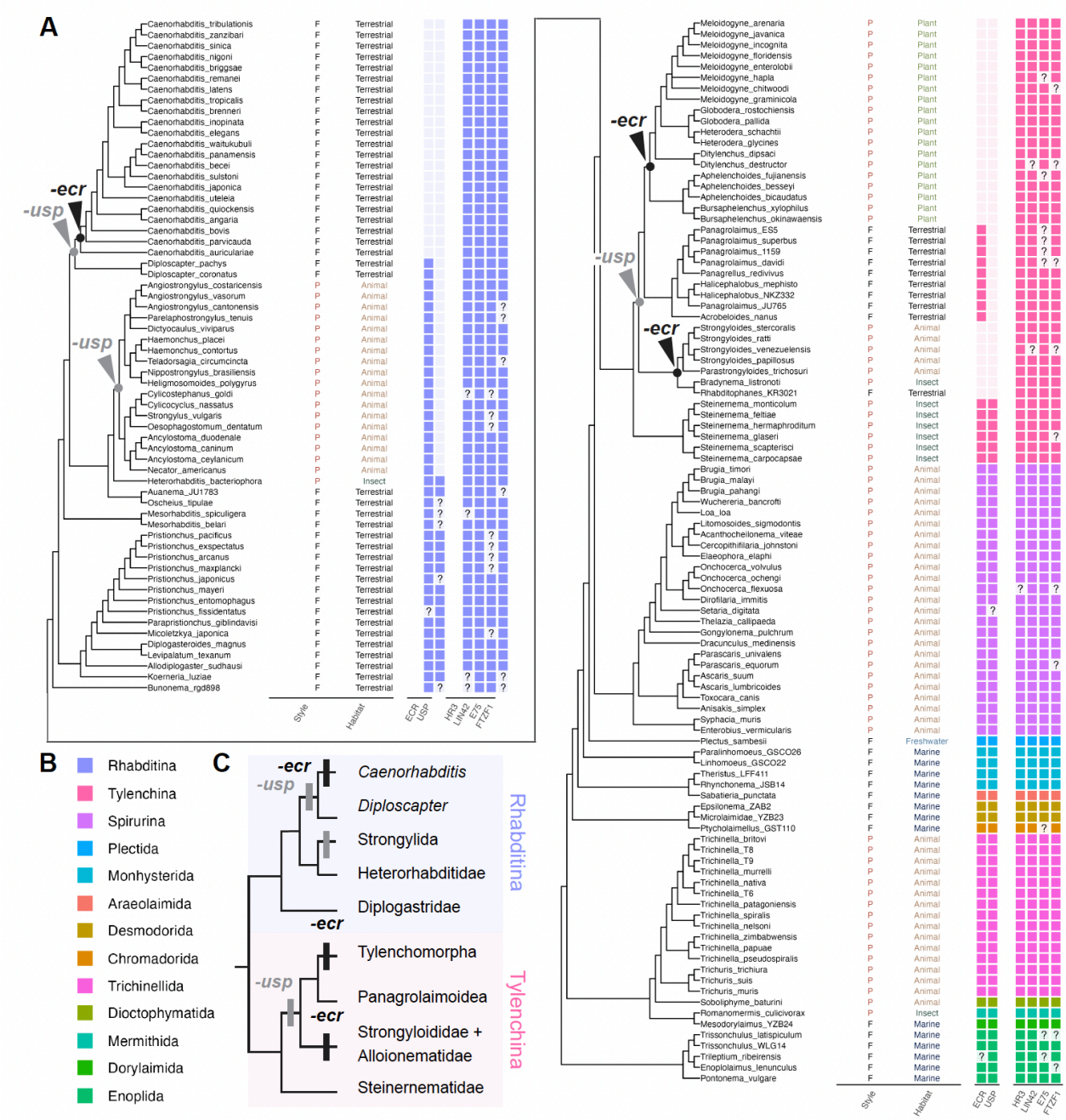

Figure 2. Gene repertory of the target genes (*ecr, usp, hr3, lin-42, e75, and ftz-f1)* in 160 nematode species A: Lifestyle (P: parasite and F: free-living), habitat, and gene repertories (*ecr, usp, hr3, lin-42, e75, and ftz-f1*) are indicated with the phylogeny of the target nematode species (color represents the taxa, question marks represent missing information). The nodes of *ecr* and *usp* loss events are highlighted in the tree. **B**: Legends for color and taxa. **C**: A simpler tree clarifying the loss of ECR and USP in the Rhabditina and Tylenchina groups

2. Conserved temporal expression of *ecr* and *usp* during molting cycle in Trichinellida, Spirurina, and Rhabditina nematodes

To reveal how *ecr* is lost multiple times during nematode evolution, we first investigated whether *ecr* has a molting regulatory function in various nematode species. Particularly, we speculated that the function of ecdysone as a molting trigger is specifically lost in Rhabditina and Tylenchina. To test this hypothesis, we examined the temporal expression patterns of *ecr* and *usp* during the molting cycle in the representative nematodes. Previous studies have shown that molting-related genes, including *ecr*, exhibit oscillatory expression peaking just before ecdysis in various ecdysozoan species (Gao, et al. 2015; Liu, et al. 2022; Yamakawa and Hejnol 2024). Based on this, we used the temporal expression of *ecr* during the molting cycle as an indicator of its involvement in molting regulation.

We examined the temporal expression of *ecr* during the molting cycles of four nematode species (Fig. 3A, B, Rhabditina: *Pristionchus pacificus*, *Ancylostoma ceylanicum*, Spirurina: *Brugia malayi*, and Trichinellida: *Trichuris suis*), for which transcriptome data during the molting cycle are publicly available (see methods). In *T. suis*, *ecr* expression showed a sharp peak pattern before L3-L4 and L4-adult molting (Fig. 3B). Similar (but more moderate) peaked expression was observed in L3-L4 molting of *B. malayi* (Fig. 3B), and these expression patterns are consistent with the molting trigger function of ecdysone/ECR. On the other hand, although a pulsed expression of *ecr* was detected in L2-L3 and L3-L4 molting of *P. pacificus*, the expression peaks did not precede a start of molting but showed at the same time (or later) as ecdysis, a final step of molting (Fig. 3B, see also the method and Fig. S6). Furthermore, the expression of *ecr* in *A. ceylanisum*, which lacks *usp*, showed a comparatively minor increase during L3-L4 molting (Fig. 3B).

We also investigated the expression of *usp* genes in three species which possess *usp* (Fig. 3A, C: *P. pacificus*, *T. suis*, and *B. malayi*). Similar to *ecr*, *usp* also shows a peaked expression pattern before molting in *T. suis* and *B. malayi* (Fig. 3B). The temporal expression of *ecr* and *usp* is similar in both species (Fig. 3B–D), which is consistent with the ECR-USP function in triggering molting. *usp* of *P. pacificus* also shows comparatively correlated expression with *ecr* (Fig. 3B–D). Although the correlation is less clear than in *T. suis* and *B. malayi* (Fig. 3B–D), it is still plausible that *ecr* and *usp* are involved in molting process of *P. pacificus*. Similar expression of *P. pacifucs ecr* and *usp* was previously observed during molting cycles in a semi-quantitative PCR analysis (Ppa-pnhr2 and Ppa-pnhr-1, respectively, 3–48 hours after hatching with a three-hour interval) (Parihar, et al. 2010).

In summary, it is plausible to interpret that ECR and USP are involved in molting regulation in Trichinellida, Spirurina, and some Rhabditina nematodes (e.g., *P. pacificus*), all of which possess both *ecr* and *usp* genes. However, our data also suggest that the molting trigger function of ECR is lost in parallel with the loss of *ecr* and *usp*.

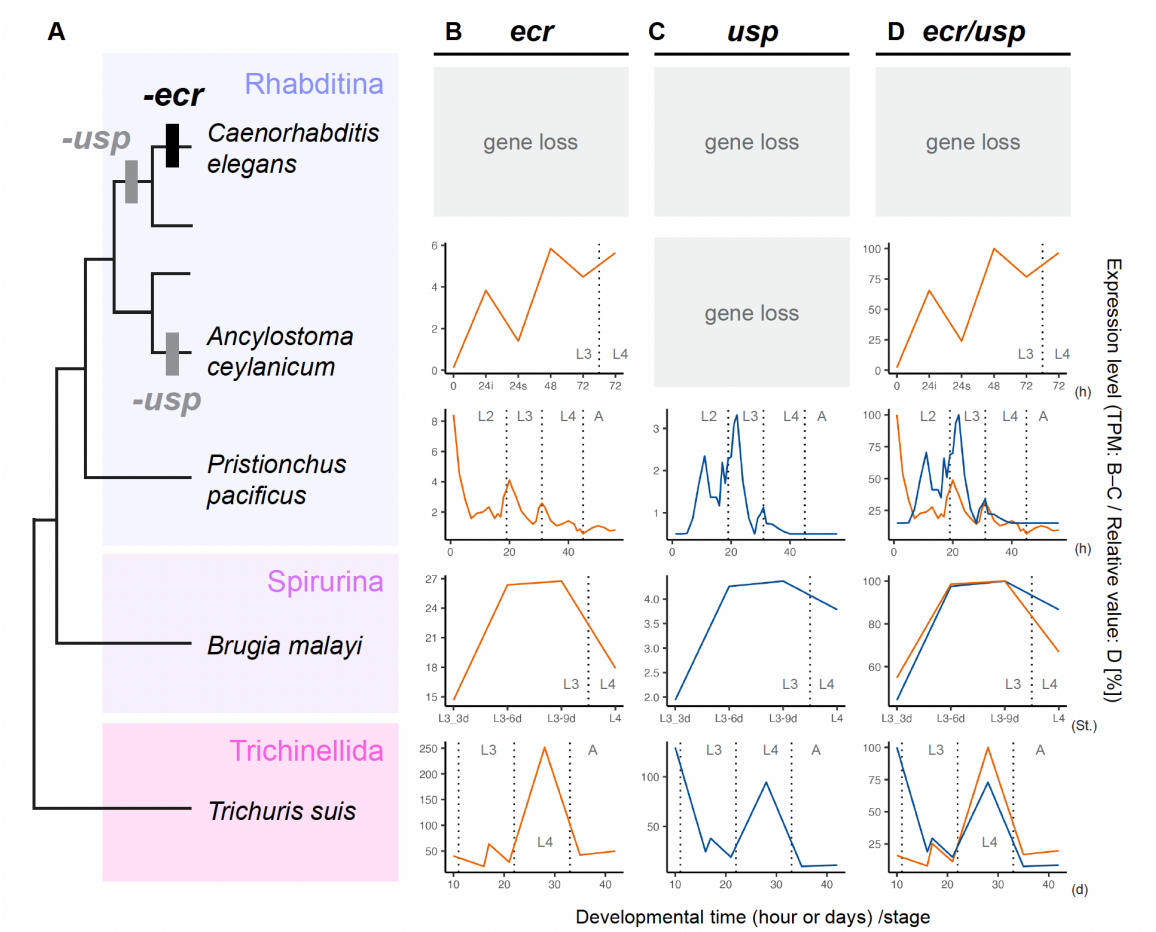

Figure 3. Temporal expression pattern of *ecr* and *usp* during the molting cycle in the representative nematode species

A: Phylogeny of the target nematode species and occurrence of *ecr* and *usp* loss events. **B**–**D**: Temporal expression patterns of *ecr*, *usp,* and both genes, respectively. The x-axis indicates developmental time (hours/h, days/d, or stages/St.), and the y-axis shows expression levels (transcripts per million [TPM] in **B** and **C** and relative expression level [%] in **D**). The vertical dotted lines indicate the timing of molting or ecdysis (L1–L4: first to fourth larval stages; A: adult stage).

3. Identification of putative conserved molting regulators among nematodes

Although we found the putatively divergent molting function of ECR, the molting process itself appears consistent across nematodes despite such differences (e.g., most nematodes consistently molt four times (Malakhov 1986)). This suggests the presence of other key regulators. Thus, building on our knowledge of *C. elegans* molting regulation (Fig. 1C), we sought to identify conserved regulators across nematodes. Specifically, we focused on the four representative regulators (Fig. 1C): *hr3* (*nhr-23*), *lin-42* (*per*), *e75* (*nhr-85*), and *ftz-f1* (*nhr-25*).

First, our survey revealed that all genes are highly conserved across nematode lineages (Fig. 2A). Only *e75* genes may be lost in some *Pristionchus* and *Panagrolaimus*

lineages (Fig. 2A). We then examined the expression pattern of the four genes during the molting cycle in six nematode species (Fig. 4, the above four species, *ecr*-lacking Rhabditina *C. elegans*, and *ecr*-lacking Tylenchina *Globodera pallida*). Notably, pulsed expression of *hr3* prior to molting was observed in all six species (Fig. 4B). For example, *hr3* expression shows a peaked pattern prior to molting in *A. ceylanisum* which does not show peaked *ecr* expression, and *G. pallida* which lacks *ecr* (Figs 3B, 4B). A similar expression pattern was observed in *lin-42* of *C. elegans*, *A. ceylanicum*, *P. pacificus*, and *B. malayi* (Fig. 4C). However, this pattern was not observed during the molting process of *G. pallida* and *T. suis* (Fig. 4C). The temporal expression patterns of *e75* and *ftz-f1* are also not conserved among the six species examined (Fig. 4D, E). Therefore, we concluded that HR3 is a promising candidate for an evolutionary conserved regulator of nematode molting.

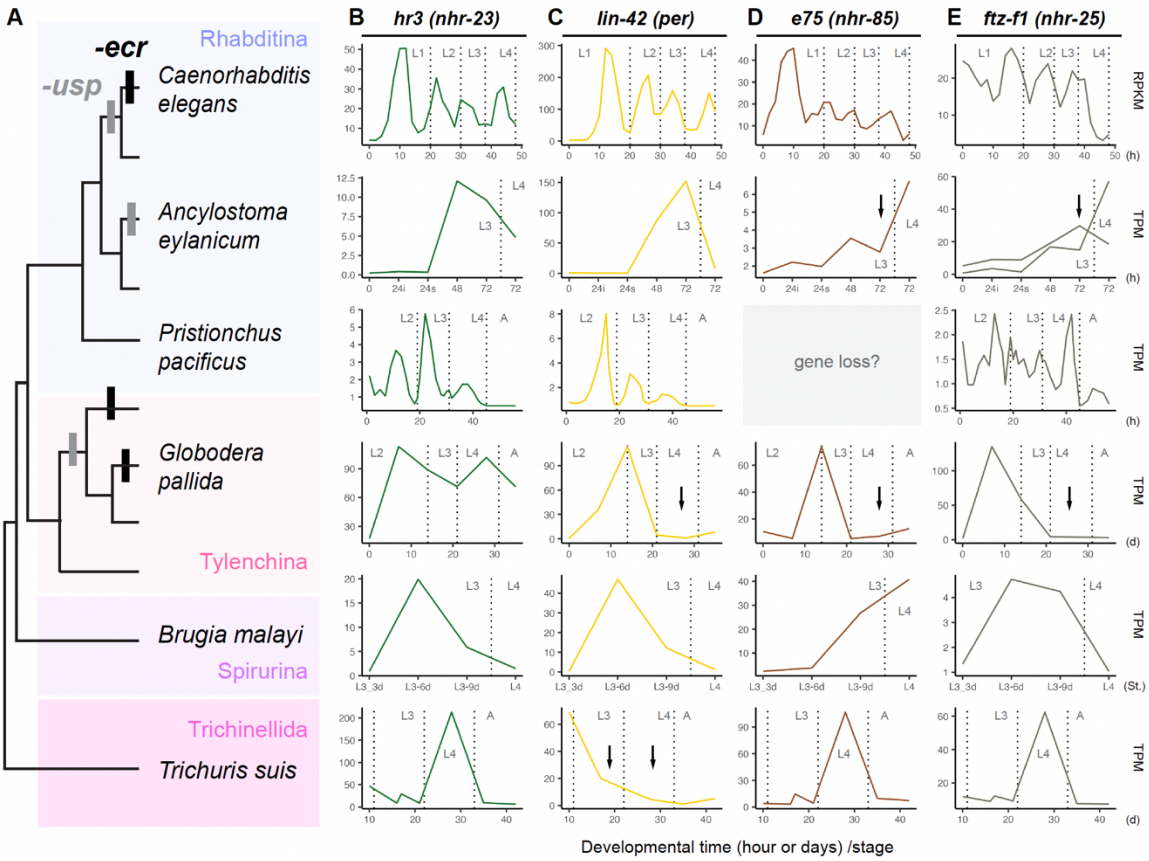

Figure 4. Temporal expression pattern of *hr3*, *lin-42*, *e75,* and *ftz-f1* during the molting cycle in representative nematode species

A: Phylogeny of the target nematode species and occurrence of *ecr* and *usp* loss events. **B**–**E**: Temporal expression patterns of *hr3/nhr-23*, *lin-42/per, e75/nhr*-85, and *ftz-f1/nhr-25* genes, respectively. The x-axis indicates developmental time (hours/h, days/d, or stages/St.), and the y-axis shows expression levels (transcripts per million [TPM] in **B** and **C** and relative expression level [%] in **D**). The vertical dotted lines indicate the timing of molting or ecdysis (L1–L4: first to fourth larval stages; A: adult stage). The arrows indicate that there was no increased or peaked in expression just before molting/ecdysis.

We also performed systematic and unbiased screening of the candidate genes of conserved molting regulators across the above six species. Previously, the genes showing oscillatory expression during the molting cycle were extracted from *C. elegans* (1,592 genes) and *P. pacificus* (2,964 genes) (Kim, et al. 2013; Sun, et al. 2021). For the remaining four species, we performed a fuzzy c-mean clustering analysis on each transcriptome dataset and extracted the cluster(s) showing peaked expression just before molting in each species (Fig. S7; green shades; *A. ceylanicum*: 8,110; *G. pallida*: 3,383; *B. malayi*: 7,114; and *T. suis*: 2,896 genes). Then, we used OrthoFinder to extract orthologous groups (OGs) among the screened genes (Emms and Kelly 2019). Of the total 5,180 OGs identified, we found that 55 OGs contain one or more genes from all species. For example, a total of 168 *C. elegans* genes were assigned to any of the 55 OGs (Table S1). The genes involved in cuticle development were included in the 55 OGs (e.g., nematode cuticle collagen [col-125, col-33, col-133/OG0000005]), supporting the feasibility of our screening for molting regulatory genes. Finally, we searched for transcription factor genes among 168 *C. elegans* genes, based on their domain structure. We found that only three OGs include transcription factor genes. Notably, although molting regulatory functions have not been reported in two OGs (OG0000071/Homeobox: *lin-39* and *nob-1*; OG0000130/zf-C2H2: *sptf-2* and *znf-782*), our screening results included *hr3* (OG0000063/Hormone_receptor, zf-C4). No other nuclear receptor genes were identified as candiadte genes from this screening.

In conclusion, our candidate-based approach and unbiased screening both support the evolutionary conserved role of *hr3/nhr-23* in nematode molting. This gene potentially buffers the loss of multiple ECR genes and their functions.

4. Extensive expansion of nuclear receptors which may underlie the loss of *ecr* and *usp*

We finally aimed to understand why *ecr* and *usp* are lost specifically in Rhabditina and Tylenchina. In particular, we focused on the pleiotropic functions of the ecdysone/ECR which are suggested in nematodes (e.g., reproduction) (Barker and Rees 1990). USP is also expected to play various roles that are different from the regulation of molting since USP (or RXR) functions as a heterodimer partner with different NRs (Pérez, et al. 2012). Thus, it is plausible that not only *hr3* but different genes may also buffer or even take over the ECR and USP function in *ecr/usp*-lacking species. In this context, it is interesting that Rhabditina and Tylenchina species extensively expanded nuclear receptor (NR) genes (Sural and Hobert 2021). In the following, we investigated the relationship between NR expansion and ECR/USP losses.

Stepwise expansion of nematode NRs

We first identified the NRs by extracting the proteins having NR conserved domains from 160 nematode species. Plotting the number of NRs in the phylogenetic tree shows that NR expansion proceeded in a stepwise manner under phylogenetic constraints (Fig. 5A). We then extracted orthogroups (OGs) of NRs from represented 11 species (1–3 species from each Rhabditina, Tylenchina, Spirurina, Trichinellida, and Enoplida; Figs 5, S8). This analysis showed that the common ancestor of nematodes has at least 12 OGs, and NRs

increased to 34 OGs in the ancestor of Rhabditida (Figs 5A, B, S8: Spirurina/Rhabditina/Tylenchina). Finally, the ancestor of Rhabditina/Tylenchina acquired additional 22 OGs (total 56 OGs), and Rhabditina and Tylenchina ancestrally had 136 and 75 OGs, respectively (Figs 5A, B, S8). Some nematodes such as *Plectus sambesii* also increased NRs (Fig. 5A), while *ecr* and *usp* are not missing. Thus, although expansions of NRs did not strictly correlate with the loss of *ecr* and *usp* in some lineages, it is plausible that Rhabditina and Tylenchina are unique to have abundant "resource" to take over ECR and USP function.

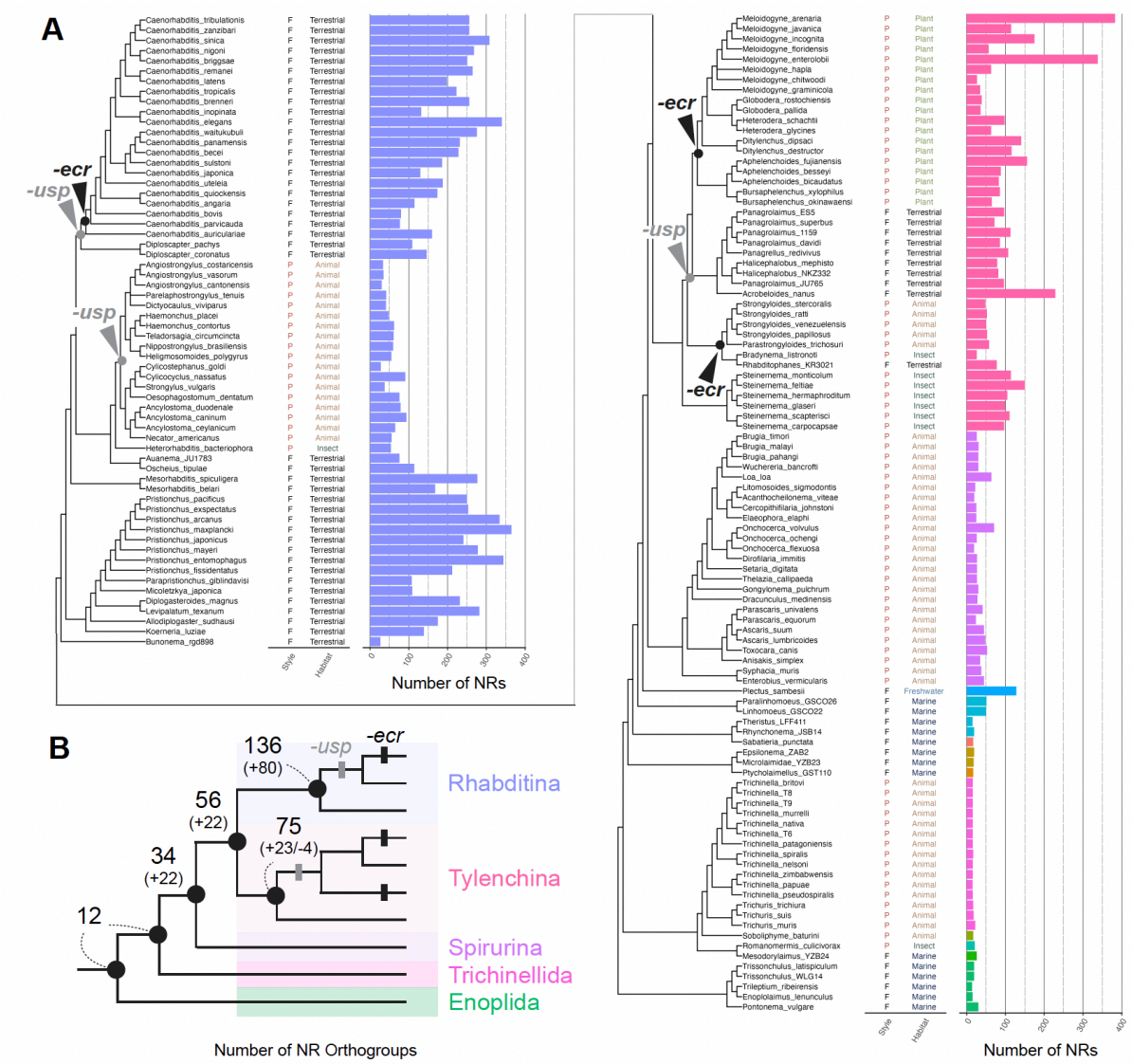

Figure 5. The evolutionary process of expansion of nematode nuclear receptors
A: Lifestyle (P: parasite and F: free-living), habitat, and the number of nuclear receptors (NRs) are indicated in the phylogeny of the target nematode species (color represents the taxa, see Fig. 1B). The nodes of *ecr* and *usp* loss events are highlighted in the tree. **C**: a simpler tree indicating the increase of NR orthogroups (OGs) at the nodes of representative taxa. The number above shows

296 the number of OGs, and the number in the brackets below shows the increase (+) or decrease (-) of
297 OGs at each node.
298

299 It should be notified that HNF4 subtype genes, the same NR subfamily with USP,
300 are extensively expanded in nematode (Bonneton, et al. 2008; Kostrouchova and Kostrouch
301 2015). Thus, it can be suggested that the heterodimer function of USP can be readily taken
302 over. Indeed, changes in NR heterodimer functionality was proposed in *C. elegans*
303 (Kostrouchova and Kostrouch 2015), with emergence of novel heterodimer pairs within
304 expanded NRs (e.g., NHR-80 and NHR-49) (Pathare, et al. 2012). In this study, we showed
305 that loss of *ecr* occurs only in the lineages lacking *usp* (Fig. 2A), suggesting that the loss
306 of USP heterodimer is an important step towards the loss of *ecr*. This aspect of NR
307 expansion likely underlies the specific loss of ECR within Rhabditina and Tylenchina
308 across nematodes.

309

310 *Evolutionary changes of heterodimer functionality of nematode HNF4s*

311 Our hypothesis predicts that, although some expanded NRs are derived from HNF4-
312 subtype NRs, they have acquired structural and functional features similar to those of ECRs
313 or USPs. We performed *in silico* screening to identify such proteins and support our
314 hypothesis. Specifically, we aimed to identify HNF4s with USP-like functions in
315 nematodes lacking *usp*, based on the well-suported premise that these heterodimeric
316 features can be detected using the latest AI-based prediction of protein structural
317 interactions.

318 First, we searched for NRs with a structural feature similar to USP in the model
319 nematode *C. elegans* using the Foldseek search tool (van Kempen, et al. 2024). The ligand-
320 binding domains of ECR and USP have been experimentally determined to form a
321 heterodimer (Hill, et al. 2013; Browning, et al. 2021). Thus, using the ligand-binding
322 domain of the USP protein from *D. melanogaster* as the query, we searched the AFDB-
323 proteome database of *C. elegans* (UP000001940). As a result, we identified five candidate
324 NRs with the top hit score (Table S2: NHR-64, NHR-69, NHR-35, NHR-14, and NHR-
325 49). By investigating the presence of these proteins in other nematode species, we
326 confirmed that all five proteins evolved from the NHF4 NR subtype within nematodes
327 (=expanded HNF4s, Figs 6A, S9). Interestingly, NHR-49 is known to have evolved the
328 ability to form a heterodimer with different expanded NRs, as mentioned above (Pathare,
329 et al. 2012). Assuming similar structural evolution occurs in our other target proteins, we
330 investigated their structural functionality.

331 We used the ColabFold tool with AlphaFold2-Multimer to test if our target proteins
332 could form a heterodimer with ECR (Jumper, et al. 2021; Evans, et al. 2022; Mirdita, et al.
333 2022). First, we validated that the ECR-USP heterodimer structure is correctly predicted
334 in *Drosophila melanogaster*. The predicted structural alignment of the ECR-USP
335 heterodimer is highly consistent with the experimentally determined ECR-USP
336 heterodimer (Fig. 6B) (Hill, et al. 2013; Browning, et al. 2021), and the ipTM (interface
337 predicted template modeling) score is greater than 0.9. Furthermore, the PAE (predicted

alignment error) heatmap clearly shows the high certainty of each ECR and USP prediction (Fig. 6B, second and fourth quadrants) as well as the interaction of ECR and USP (Fig. 6B, first and third quadrants). Conversely, a high-probability heterodimer interaction was not predicted when testing ECR and HNF4, which heterodimer functions have not been reported in *D. melanogaster* (Fig. 6C, ipTM = 0.15). The PAE heatmap shows that the interface of ECR and HNF4 is not accurately predicted (Fig. 6C; high error ratio [red color] in the first and third quadrants), suggesting that the predicted alignment is likely due to random coincidence (Evans, et al. 2022). Thus, this analysis proved to be effective in identifying heterodimeric pairs of ECR.

We tested whether each candidate protein (NHR-64, NHR-69, NHR-35, NHR-14, and NHR-49) forms a heterodimer with *D. melanogaster* ECR. As shown in the analysis of ECR and HNF4 in *D. melanogaster*, heterodimer interaction was not clearly detected for three of the five proteins (Fig. S10: NHR-35, NHR-14, and NHR-49; piTM = 0.209, 0.68, and 0.166, respectively). Notably, however, our results clearly predicted that NHR-64 and NHR-69 form a heterodimer with ECR (Fig. 6D, I, ipTM = 0.805 and 0.887, respectively). The structure of the putative heterodimer resembles that of the *D. melanogaster* ECR-USP heterodimer (Fig. 6B, D, and I). Furthermore, not only *C. elegans* but other Rhabditina and Tylenchina nematodes have orthologs of NHR-69 and NHR-64 that exhibit similar structural features (Fig. 6E: *Globodera pallida* NHR-69 [ipTM = 0.878]; Fig. 6H: *Pristionchus pacificus* NHR-64 [ipTM = 0.846]; and Fig. S11B: Other examples). Our analysis also predicted that *C. elegans* NHR-69 and NHR-64 can form a heterodimer with ECR of the nematode *Brugia malayi* (Fig. S11C).

Finally, we investigated the structural feature of "ancestral" HNF4 proteins, which evolved before the expansion of NRs and are conserved in some nematodes such as Enoplida and Trichinellida (Figs 6A, F, G, and J and S11A). Interestingly, such HNF4s were not predicted to interact with ECR heterodimers (Fig. 6F: *Pontonema vulgare* [ipTM = 0.241]; Fig. 6G: *Trichuris muris* [ipTM = 0.181]; Fig. S11A: other examples). This is similar to the results of the ECR-HNF4 comparison in *D. melanogaster* (Fig. 6C). Taken together, our analyses showed that some HNF4s evolved distinct structural features for dimerization during the NRs/HNF4s expansion within nematodes. These results are consistent with our hypothesis that expanded NRs took over the function of USP.

(Next page) **Figure 6. The evolution of the heterodimer functionality of nematode HNF4 genes during NR expansion events**

A: Evolutionary origin of the target proteins (NHR-64, NHR-69, NHR-35, NHR-14, and NHR-49) in the nematode phylogeny, with ECR and USP loss events highlighted. **B**–**I**: 3D models, ipTM values, and PAE heatmaps of the highest-scoring predicted heterodimer structure. All target proteins were investigated with ECR from *Drosophila melanogaster* (DmECR). **B**: *D. melanogaster* USP (DmUSP), **C**: *D. melanogaster* HNF4 (DmHNF4), **D**: *Caenorhabditis elegans* NHR-64 (CeNHR-64), **E**: *Globodera pallida* NHR-64 (GpNHR-64), **F**: *Pontonema vulgare* HNF4 (PvHNF4), **G**; *Trichuris murris* HNF4 (TmHNF4), **H**: *Pristionchus pacificus* NHR-69 (PpNHR-69), and **I**; *Caenorhabditis elegans* NHR-69 (CeNHR-69). The ipTM values and PAE heatmaps are shown below the 3D models. **J**: Phylogenetic tree of four species (*P. vulgare*, *T. muris*, *P. pacificus*, and *C. elegans*) showing the origin of HNF4 and NR expansion and loss of USP.

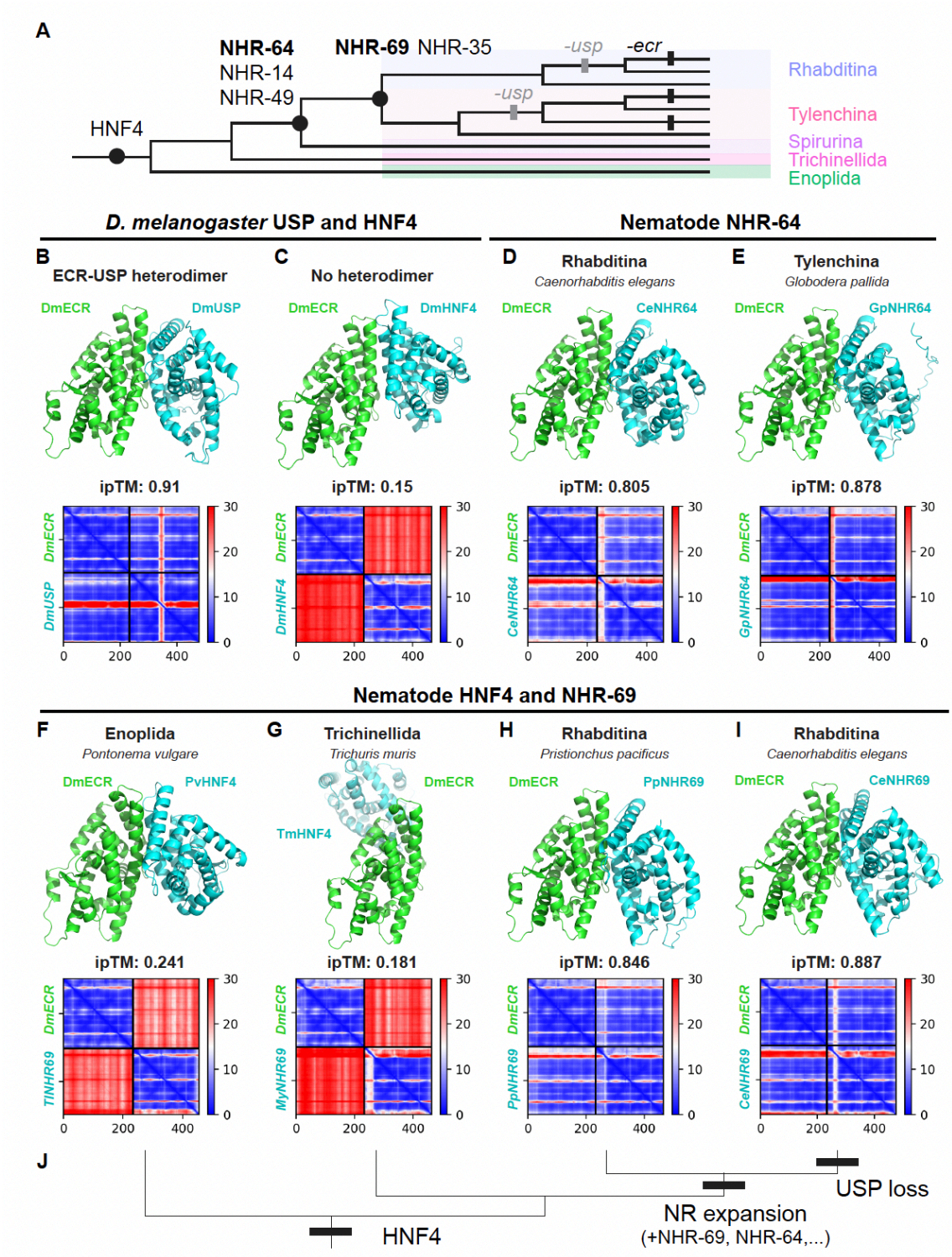
A
NHR-64
NHR-14
NHR-49
NHR-69 NHR-35
-usp
-ecr
-usp
HNF4
Rhabditina
Tylenchina
Spirurina
Trichinellida
Enoplida
D. melanogaster USP and HNF4
Nematode NHR-64
B
ECR-USP heterodimer
DmECR
DmUSP
ipTM: 0.91
C
No heterodimer
DmECR
DmHNF4
ipTM: 0.15
D
Rhabditina
Caenorhabditis elegans
DmECR
CeNHR64
ipTM: 0.805
E
Tylenchina
Globodera pallida
DmECR
GpNHR64
ipTM: 0.878
Nematode HNF4 and NHR-69
F
Enoplida
Pontonema vulgare
DmECR
PvHNF4
ipTM: 0.241
G
Trichinellida
Trichuris muris
DmECR
TmHNF4
ipTM: 0.181
H
Rhabditina
Pristionchus pacificus
DmECR
PpNHR69
ipTM: 0.846
I
Rhabditina
Caenorhabditis elegans
DmECR
CeNHR69
ipTM: 0.887
J
USP loss
NR expansion
(+NHR-69, NHR-64,...)
HNF4

382

Discussion

This study found that loss of *ecr* and *usp* is not unique to *Caenphrabditis* but has occurred multiple times within nematodes. We also suggest that molting regulation by an alternative regulator and the expansion of NRs may explain why *ecr* and *usp* are specifically lost within Rhabditina and Tylenchina species. Based on our findings, we proposed an evolutionary scenario of molting regulation in nematodes (Fig. 7).

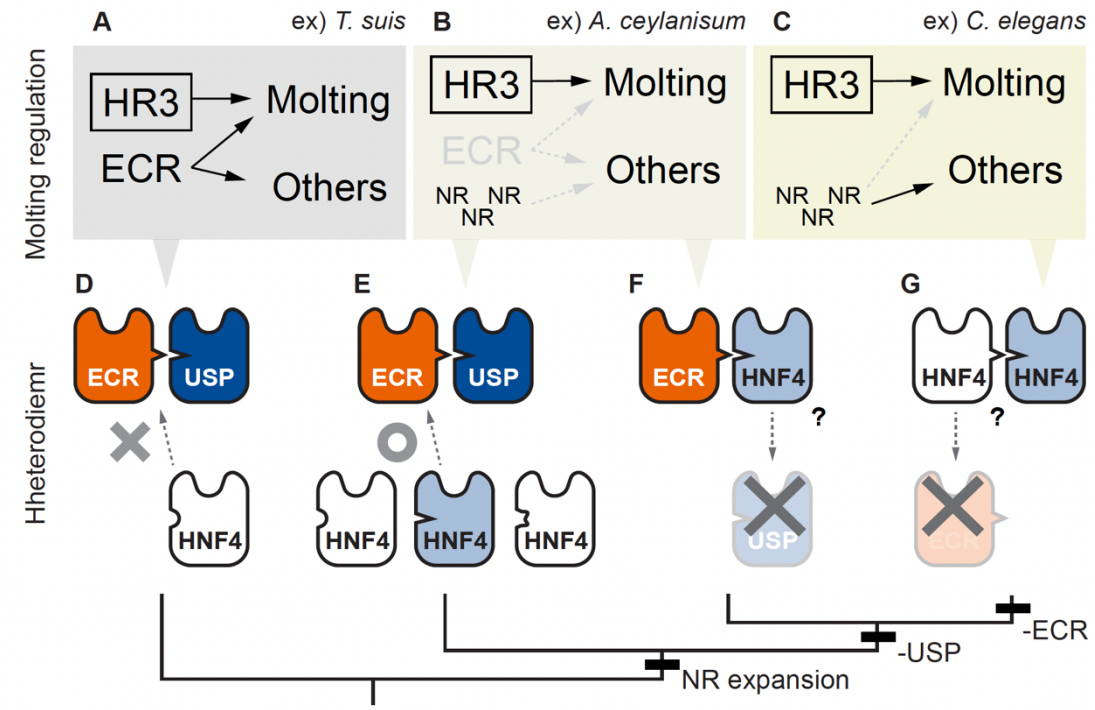

Figure 7. Hypothetical evolutionary process behind the multiple losses of *ecr* and *usp* in nematodes

A–**C**, **D**–**G**: Hypothetical evolutionary changes in the molting regulatory machinery and heterodimer functionality during nematode evolution, respectively. **A**–**C**: Molting regulation may be ancestrally dependent on ecdysone/ECR signaling and HR3/NHR-23 (**A**). ECRs likely have also other developmental functions (**A**). After the expansion of NRs, such functions (**B**) and finally ECR itself (**C**) are lost buffered by the expanded NRs. HR3 may play core regulatory roles (shown by the square) and may also buffer the loss of ECR. **D**–**G**: HNF4 cannot form a heterodimer with ECR ancestrally (**D**); however, the new structural functionality evolved in expanded HNF4 proteins to make a heterodimer with ECR (**E**). This redundancy in ECR heterodimers may lead to the loss of USP (**F**) and, eventually, ECR (**G**).

Evolutionary scenario of nematode molting regulation

Based on the previous reports in Spirurina parasitic nematodes and our transcriptome analysis (Fig. 3), it is well-supported that ecdysone is ancestrally involved in the regulation of nematode molting. Additionally, this study suggests that HR3/NHR-23 plays a regulatory role in molting across nematode taxa. Given that *hr3* and its expression is highly conserved regardless of *ecr* and *usp* loss (Figs 2A and 4B), HR3 may play a "major"

regulatory role in nematode molting (Fig. 7A–C). Note that some components of *C. elegans* molting regulation, such as Lin-42, also show a conserved expression pattern during molting cycle among different nematodes (Fig. 5). This suggests that not only HR3 but also other genes may be also involved in the molting of nematode ancestors. With such regulatory machinery, the loss of *ecr* and *usp* may be buffered without causing catastrophic effects on the molting process itself.

As exemplified by our findings regarding the structural evolution of HNF4 proteins (Fig. 6), we hypothesized that changes in NR functionality also underlie the loss of ECR and USP in Rhabditina and Tylenchina (Fig. 7D–G). Our findings suggest that the redundancy of NR heterodimeric partners emerges through NR/HNF4 expansion (Fig. 7D, E). For example, some Rhabditina nematode species have both USP and HNF4s having USP-like heterodimeric functionality (e.g., *Pristionchus pacificus*, Figs 6H, 7E). We suggest that such lineages likely represent an ancestral state of Rhabditina and Tylenchina, and the loss of *usp* may happen comparatively easily within them (Fig. 7F). This condition may also lead to the evolution of novel NR heterodimer pairs (Fig. 7G), examplified by NHR-49 and NHR-80 in *C. elegans* (Pathare, et al. 2012). It is also interesting that the ECR of *Haemonchus contortus* (Rhabditina without *usp*) cannot form heterodimers with the USP of the red louse *Bovicola bovis* (Graham, et al. 2010), suggesting that the functionality of ECR may also be altered in parallel with the NR expansion. While this study does not directly address how ECR is lost in lineages lacking USP (Fig. 7G), we suggest that the loss of ECR may also be driven by changes in NR interactions.

Other remarks on our hypothesis

Further assessment of our hypothesis requires experimental support. In particular, we suggest testing two important aspects in future studies. First, ecdysone-dependent molting must be clearly demonstrated at the gene function level in nematodes. Beyond a pharmacological and hormone quantification assay, the regulatory roles of *ecr and usp* need to be demonstrated at the level of gene function in various nematodes. The occurrence of ecdysone synthesis and the identification of the synthesis gene machinery are also necessary. The role of *hr3/nhr-23* in regulating molting must also be demonstrated at the gene level in various nematode species. Recently, gene function assays have gradually been established in several non-model nematode species, such as *Auanema*, *Steinernema*, and *Panagrolaimus* (Adams, et al. 2019; Cao 2023; Hellekes, et al. 2023). This methodological development paves the way for comparative research across nematode species.

Second, while this study showed that NHR-64 and NHR-69 have structural similarities with USP (Fig. 6), it remains unclear whether these receptors are responsible for buffering the loss of USP function in nematode evolution. Previous studies have reported that NHR-64 and NHR-69 are involved in fat storage and insulin secretion, respectively (Liang, et al. 2010; Park, et al. 2012). For example, NHR-69 interacts with DAF-8 (R-Smad) to regulate insulin secretion and dauer formation (Park, et al. 2012). These functions are thought to be conserved among bilaterians (Liang, et al. 2010; Park, et al. 2012; Fasteen, et al. 2025), rather than any biological functions likely regulated by ecdysone signaling (e.g., molting). Nevertheless, we would like to note that this does not

450 necessarily contradict our hypothesis. For example, considering that USP (or RXR) has
451 various functions as a heterodimer partner (Pérez, et al. 2012), NHR-64 and NHR-69 may
452 have taken over only some of USP's functions. It is also interesting that NHR-69 is
453 expressed not only in the digestive organs, but also in the hypodermis cells where the
454 cuticles are synthesized (Gissendanner, et al. 2004). Alternatively, other NR/HNF4s may
455 evolve novel structural features and dominate USP function. In any case, in addition to a
456 detailed analysis of NHR-64 and NHR-69, comprehensive research charactering expanded
457 NRs and revealing the evolutionary impacts of the NR expansion event are critical. For
458 example, investigating the divergence of ligand-binding affinity may identify HNF4s
459 which have an ECR-like ligand-binding domain.

460

461 *Insights into evolution of NR expansion and ecdysozaon molting*

462 The expansion of nematode NRs has been regarded as a "natural experiment made by a
463 phylum" (Kostrouchova and Kostrouch 2015), and its evolutionary significance has been
464 widely studied (Taubert, et al. 2011; Antebi 2015; Kostrouchova and Kostrouch 2015;
465 Sural and Hobert 2021). For example, Sural and Hobert (2021) proposed that the expansion
466 of NRs is correlated with a free-living lifestyle. They reported that the expression of NRs,
467 GPCRs, and insulin genes is enriched in the sensory neurons of *C. elegans* (Sural and
468 Hobert 2021). Based on the findings, they hypothesizes that NRs may integrate sensory
469 and/or internal information (Sural and Hobert 2021). It has also been suggested that NRs
470 expanded in response to xenobiotics in free-living nematodes (Lindblom, et al. 2001;
471 Lindblom and Dodd 2006). Notably, various other functions have been reported in addition
472 to these examples (Taubert, et al. 2011; Antebi 2015; Kostrouchova and Kostrouch 2015).
473 In this study, we found that NR expansion proceeded in a stepwise manner under
474 phylogenetic constraints (Fig. 5) and that NR evolved novel structural features (Fig. 6). We
475 would like to discuss that our findings are not contradictory to previous research. For
476 example, some parasitic lineages lost many NRs after the expansion of NRs in Rhabditina
477 (Fig. 5A), which supports the correlation between NR expansion and a free-living lifestyle
478 in this group. Additionally, our findings about changes in NR structural features shows
479 affinity with the divergence of NR functions. We propose that changes in NR functionality,
480 including heterodimeric potential, may be a driving force behind divergent NR functions
481 in nematodes.

482 Our findings shed new light on the understanding of ecdysozoan molting.
483 Specifically, this study opens the hypothesis that HR3 plays a dominant role as an ancestral
484 and conserved molting regulator in nematodes and possibly even in ecdysozoans (note that
485 HR3 is also a core molting regulator in arthropods (Yamanaka, et al. 2013) and putatively
486 in tardigrades (Yamakawa and Hejnol 2024)). HR3 is also highly conserved among
487 ecdysozoan species (Fig. S5). Considering that HR3 orthologues ROR and NHR-23 are
488 known to be involved in regulation of circadian clocks among bilaterians (Patke, et al.
489 2020; Hiroki and Yoshitane 2024; Patil and van Zon 2024), the ancestry of HR3 shows a
490 correlation with the origin of molting regulation, which control biological and
491 developmental time. Our results also provide the possible use of HR3 regulation of molting

492 for medical applications and pest control, in plant-parasitic and some human-parasitic
493 nematodes, which have lost ECR (Fig. 2A: Tylenchomorpha and Strongylida,
494 respectively).

495

496 **Materials and Methods**

497 **1. Data collection and target species**

498 We obtained protein sequences of 159 nematode species from WormBase Parasite
499 (version: WBPS19, WS291) (Howe, et al. 2017). These sequences/protein models were
500 reconstructed from the genomic data. All accession numbers of the original dataset are
501 available in the supplementary dataset. In this study, the gene ID was referenced to the
502 original dataset, while also incorporating some modifications. For example, species
503 identifiers were added to the beginning of the gene ID (i.e. *GeneID* →
504 *NEMA_CaenoElega_GeneID*). Some characters, such as curly brackets, were also
505 removed for later analysis. In addition, the transcriptome data of the Enoplida nematode
506 *Pontonema vulgare* was obtained from NCBI (accession number: PRJNA504396). Quality
507 of raw reads were examined using FastQC (version:
508 v0.11.9; https://www.bioinformatics.babraham.ac.uk/projects/fastqc/). The subsequent
509 filtering was performed using trimmomatic (version: 0.39) (Bolger, et al. 2014), and *de*
510 *novo* assembly was conducted using Trinity (version: v2.13.2) (Henschel, et al. 2012).
511 Transdecoder (version: 5.5.0; https://github.com/TransDecoder/TransDecoder) was used
512 to obtain the peptide sequences of *P. vulgare* transcript models. The assembled sequences
513 are available in the supplementary dataset.

514 The phylogenetic relationship of the target species was referenced to previous
515 studies. For example, the topology of the major taxon phylogeny (grouped by color in Fig.
516 2) is consistent with three recent molecular phylogenetic reports (Smythe, et al. 2019;
517 Ahmed, et al. 2022; Qing, et al. 2024). Since the analysis by Ahmed et al. (2022) used the
518 largest number of our target species, we reconstructed the phylogenetic relationship of our
519 target species with primarily following their tree. If our target species were not included in
520 their analysis, we referred to other literature. For example, we used Ahmed et al. (2022) to
521 reconstruct the phylogeny of *Caenorhabditis* species, but the position of *C. auriculariae*
522 was unclear in that study. In this case, we determined the position of *C. auriculariae* based
523 on another study (Dayi, et al. 2021). The phylogenetic positions of the following species
524 were determined not only with reference to Ahmed et al., 2022: *Angiostrongylus*
525 *cantonensis* (Dumidae, et al. 2023), *Cylicocylus radiatus* (Hu, et al. 2020), *Meloidogyne*
526 *chitwoodi* (Álvarez-Ortega, et al. 2019), *Steinernema hermaphroditum* (Schwarz, et al.
527 2025), *Aphelenchoides* species (Lai, et al. 2022), *Cercopithifilaria johnstoni* (McCann, et
528 al. 2021), and Enoplida species (Qing, et al. 2024). The phylogeny of the two species,
529 *Parelaphostrongylus tenuis* and *Bradynema listronoti*, was unclear. Their phylogenetic
530 positions were estimated by identifying their respective family, Metastrongylidae and
531 Allantonematidae, from the NCBI Taxonomy database
532 (https://www.ncbi.nlm.nih.gov/taxonomy). A Newick file for visualizing the phylogenetic
533 tree is available in the supplementary dataset.

534

535 **2. Gene identification**

536 *Screening*

537 Gene mining of *ecr*, *usp, hr3, e75, ftz-f1*, and *lin-42* was conducted based on the sequence
538 similarity by combination of BLAST search and phylogenetic analysis with the following
539 screening. All sequences and phylogenetic trees are available in the supplementary
540 datasets.

541 We first performed a BLAST search using the query sequences of ECR, USP, HR3,
542 E75, and FTZ-F1 from *Drosophila melanogaster* against the database of each nematode
543 species. The query sequences are from UniProt (ECR: P34021, USP: P20153, HR3:
544 P31396, E75: P17672, and FTZ-F1: P33244). The peptides showing the hit with less than
545 1E-20 e-value were extracted and used as query sequences for the second BLAST against
546 the *D. melanogaster* database. This database was built using the CDS sequences from
547 FlyBase (dmel-all-CDS-r6.45.fasta) (Öztürk-Çolak, et al. 2024). For the screening of LIN-
548 42, we used the query sequence and the database from *Caenorhabditis elegans* (UniProt
549 id: Q65ZG8). Finally, the peptides showing the reciprocal top hit with less than 1E-10 e-
550 value were extracted. Each candidate gene set of ECR, USP, HR3, E75, and FTZ-F1 (181,
551 256, 342, 196, and 199 peptides, respectively) was aligned with other known nuclear
552 receptors (NRs) from different animals (the sequences were previously used to identify NR
553 genes (Vogeler, et al. 2014; Yamakawa and Hejnol 2024) (see also the supplementary
554 dataset) using MAFFT (version: v7.526, --auto option) (Katoh and Standley 2013), and the
555 alignments were filtered using trimAl (version: 1.4.1, threshold: 0.8) (Capella-Gutiérrez,
556 et al. 2009). Candidate 203 proteins of LIN-42 were also aligned with other known Period,
557 Clock, Arnt, and Bmal proteins using the same methods (the sequences are available in the
558 supplementary dataset). Phylogenetic analysis of each data set was performed using
559 RAxML (version: 8.2.12, bootstrap: 1,000 generations, raxmlHPC-PTHREADS-SSE3 -f a
560 -x 12345 -p 12345 -# 1000 -m PROTGAMMAAUTO —-auto-prot=aic -s *input_file* -n
561 *output_file*) (Stamatakis 2014). Gene identity was determined by examining, whether the
562 candidate genes were included in the clade of target genes with high bootstrap values. By
563 removing the genes that did not belong to the target clade, we finally identified 128, 74,
564 276, 151, 199, and 132 peptide models as ECR, USP, HR3, E75, FTZ-F1, and LIN-42,
565 respectively (see the trees in the supplementary dataset). Note that some species have
566 multiple copies.

567 Next, the above identified target peptides were used as query sequences, and a
568 BLAST search was performed against the database of each nematode species in which the
569 target genes were not found in the first screening. Top-hit sequences with less than 1E-20
570 e-values were collected, and each sequence was used as a query for the second BLAST
571 search against the database of the original species from which the first query originated.
572 Then, genes showing the reciprocal one-to-one top-hit were finally accumulated as
573 candidates (ECR: 197, USP: 277, HR3: 28, E75: 77, FTZ-F1: 95, and LIN-42: 151
574 peptides). After selecting the peptides having DNA binding domain of NRs (except LIN-
575 42, HMMER domain search [version 3.4] (Johnson, et al. 2010), see the below for the
576 details) and manually checking the accuracy of the gene domain (e.g., NCBI conserved
577 domain search: https://www.ncbi.nlm.nih.gov/Structure/cdd/wrpsb.cgi), we finally
578 investigated the identity of the selected peptides by phylogenetic analysis as mentioned

above. In this analysis, 5, 21, 1, 16, 28, and 17 peptide(s) were additionally identified as ECR, USP, HR3, E75, FTZ-F1, and LIN-42, respectively. Finally, the peptides obtained in the 2nd screening were used for the BLAST query sequences, and we repeated the BLAST analysis as performed in the 2nd screening. However, no genes were newly identified as ECR, USP, HR3, FTZ-F1, and LIN-42. Only 4 peptides were additionally identified as E75.

Target genes were also searched by BLAST, Hmmer domain search (screening of the genes having DNA or ligand binding domain of NRs, see also the below), and phylogenetic analysis. For example, the BLAST search was performed with a higher e-value threshold (ex. 1E-05). Different database was also explored for the species missing the target genes, and ECR of *Steinernema feltiae* was identified using the other dataset in WormBase Parasite (version: WBPS19, WS291) from the one which we originally used (accession number: PRJNA204661). Finally, eight additional genes (nine peptides) were identified to compensate for the missing target genes, and the results are summarized in Fig. 2. Note that no *ecr* and *usp* genes were identified in the tblastn-based search on the genome assembly of the species lacking these genes.

Criteria for the presence and absence of target genes

The summary of the screening and gene identification of 160 species is shown in Fig. 2A. In some species, the target genes were missing even though the genes were found in species of the same genus (or closely related species). Since this study avoided to distinguish between species-specific loss and technical errors such as low data quality, gene missing in these species were considered as missing information in Fig. 2A (question marks in Fig. 2A). We considered the loss to be reliable if the loss of the genes was observed in all the same genus and closely related species. According to these criteria, we detected loss of *ecr* only in *Caenorhabditis*, Tylenchomorpha, Strongyloididae and Alloionematidae (Fig. 2A). Loss of *usp* was also reliable in Strongylida, Anarhabditis, non-Steinernematidae Tylenchina (Fig. 2A).

Gene identification in other ecdysozoans

Previous works identified *ecr*, *usp* and *hr3* in insects (*Drosophila melanogaster*, *Drosophila pseudoobscura*, *Anopheles gambiae*, *Aedes aegypti*, *Bombyx mori*, *Tribolium castaneum*, and *Apis mellifera*), other arthropods (Myriapoda: *Strigamia maritima*; Chelicerata: *Limulus polyphemus* and *Stegodyphus mimosarum*; and Branchiopoda: *Daphnia pulex* and *Daphnia magna*), tardigrades (*Ramazzottius varieornatus* and *Hypsibius exemplaris*), onychophorans (*Euperipatoides rowelli*), nematodes (*Brugia malayi*, *Caenorhabditis elegans* [only *hr3*]), and priapulids (*Priaplus caudutus*) (Bonneton, et al. 2008; Schumann, et al. 2018). In addition, we newly identified *ecr*, *usp*, and *hr3* in tardigrades (*Echiniscus testudo*), nematomorphs (*Acutogordius australiensis*, *Gordionus montsenyensis*, *Nectonema munidae*, *Paragordius varius*), kinorhynchs (*Campyloderes*

619 *vanhoeffeni*, *Franciscidere kalenesos*, *Dracoderes abei*) and priapulids (*Tubiluchus*
620 *corallicola*). For gene identification, we collected genomic or transcriptomic data from
621 publications or public databases (*E. testudo*: Murai et al., 2021 (Murai, et al. 2021), *A.*
622 *australiensis* and *N. munidae*: Cunha et al., 2023 (Cunha, et al. 2023) [FigShare:
623 doi.org/10.6084/m9.figshare.23419922], *G. montsenyensis*: Eleftheriadi et al., 2024
624 (Eleftheriadi, et al. 2024), *P. varius*: ERR1817116, ERR1817117, ERR1817118, and
625 ERR1817119 [NCBI SRA]; kinorhynchs: Herranz et al., 2022 (Herranz, et al. 2022) [*C.*
626 *vanhoeffeni*: SRR14509480, *F. kalenesos*: SRR14509483, and *D. abei*: SRR14509486]).
627 Raw read data from *P. varius* and kinorhynch species were *de novo* assembled as described
628 above. Gene identity was confirmed by BLAST and phylogenetic analysis using the same
629 methods as above. The results are summarized in Fig. S5, and the gene tree and sequences
630 are available in the supplemental dataset.

631

632 *Reannotation of the* ecr *genes identified by Gonzalez Akimori et al., 2021*

633 The seven ECR-1 genes used to identify ECR-1 of *Strongyloides stercoralis* in Gonzalez
634 Akimori et al. 2021 were obtained from NCBI GenBank (Gonzalez Akimori, et al. 2021).
635 The sequence of ECR-1 of *S. stercoralis* was not available due to unknown accession
636 number after their gene name modification (Gonzalez Akimori, et al. 2021). Phylogenetic
637 analysis was performed as described above, and the results are summarized in Fig. S1. We
638 also included the sequences of the ecdysozoan THR (Thyroid hormone receptor) genes
639 after preliminary test using the above dataset. All sequences for the tree are available in the
640 supplemental dataset.

641

642 *Genome assembly quality*

643 We obtained the quality metrics information for the genome assembly used in this study
644 from WormBase Parasite (version WBPS19, WS291) (Howe, et al. 2017). These metrics
645 include genome size, N50, scaffold number, BUSCO annotation score, and BUSCO
646 assembly score. These metrics are summarized in the phylogenetic trees in Figs S2–S4.

647

648 **3. Extraction of NRs and transcription factors based on the domain conservation**

649 The HMM profile of NRs (Hormone_recep: PF00104) was obtained from the Pfam
650 database. Using this profile as a query, hmmscan was performed against all peptide data of
651 the target species (threshold 1E-05) (Johnson, et al. 2010), and the identified genes were
652 considered as NRs. The number of genes was counted considering the isoforms and shown
653 in the linear bar graph of Fig. 5. We also used previously generated HMM profiles to screen
654 transcription factors (Yamakawa, et al. 2023). Shortly, the profiles include the following
655 targets: ARID (PF01388.17), AT_hook (PF02178.15), Basic (PF01586.12), CUT
656 (PF02376.11), DM (PF00751.14), Ets (PF00178.18), Forkhead (PF00250.14), GATA

657 (PF00320.23), GCM (PF03615.11), HLH (PF00010.22), HMG_box (PF00505.15),
658 Hairy_orange (PF07527.9), Homeobox (PF00046.25), Hormone_recep (PF00104.26),
659 OAR (PF03826.13), P53 (PF00870.14), P53_tetramer (PF07710.7), PAX (PF00292.14),
660 Pou (PF00157.13), HPD (PF05044.8), RHD_DNA_bind (PF00554.18), Runt
661 (PF00853.15), SCAN (PF02023.13), SIM_C (PF06621.8), SRF-TF (PF00319.14), T-box
662 (PF00907.18), TBX (PF12598.4), TF_AP-2 (PF03299.10), TF_Otx (PF03529.9), bZIP_1
663 (PF00170.17), bZIP_2 (PF07716.11), zf-C2H2 (PF00096.22), zf-C2HC (PF01530.14) and
664 zf-C4 (PF00105.14)

665

666 **4. OrthoFinder analysis**

667 OrthoFinder (version: 2.5.4, with default parameters) (Emms and Kelly 2019) was used to
668 examine the orthogroups (OGs) of NRs in the represented nematode species of five major
669 groups (Fig. 5): Rhabditina (*Ancylostoma ceylanicum*, *Caenorhabditis elegans*,
670 *Heligmosomoides polygyrus*, and *Pristionchus pacificus*), Tylenchina (*Globodera pallida*,
671 *Meloidogyne arenaria*, and *Steinernema monticolum*), Spirurina (*Ascaris suum* and *Brugia*
672 *malayi*), Trichinellida (*Trichuris muris*), and Enoplida (*Pontonema vulgare*). Peptide
673 sequences of NRs from each species were obtained as described above. After identifying
674 163 OGs in this comparison, we investigated the taxonomic origin of the genes in each OG
675 (Rhabditina, Tylenchina, Spirurina, Trichinellida, and Enoplida). If the OG contained one
676 or more genes from all taxa, the OG was considered to be the one that the common ancestor
677 of the taxa had (Fig. 5B). Using these criteria, the evolutionary gain/loss events of NR OGs
678 were resolved, as shown in Fig. 5B. Output file of the analysis is available in the
679 supplementary dataset.

680

681 **5. Transcriptome analysis**

682 *Data collection*

683 We collected transcriptome data, including molting stages, for a total of six nematode
684 species from public databases. The expression matrix (RPKM) for *Caenorhabditis elegans*
685 was obtained from Kim et al., 2013 (Gene Expression Omnibus, accession number:
686 GSE49043) (Kim, et al. 2013). WormBase ParaSite (version: WBPS19, WS291) (Howe,
687 et al. 2017) was also the resource of this study to obtain the calculated expression matrix
688 (TPM) for *Trichuris suis* (NCBI Sequence Read Archive [SRA] accession number:
689 SRP039506) and *Globodera pallida* (NCBI SRA accession number: ERP001236). The
690 expression matrix (TPM) for *Pristionchus pacificus* was obtained from the supplementary
691 file of Sun et al. 2021(Sun, et al. 2021). In addition, raw read data of *Brugia malayi* and
692 *Ancylostoma ceylanicum* were obtained from SRA (NCBI SRA, accession number:
693 SRR4308250-51 and SRR9858310-17 [*B. malayi*] (Grote, et al. 2020) and SRR2125572,
694 SRR2125581-86, SRR2125588-90, SRR2125594, SRR2125597, SRR2125600,
695 SRR2125602, SRR2125606-7, SRR2125610-SRR2125611, SRR2125614, and
696 SRR2125627 [*A. ceylanicum*] (Bernot, et al. 2020)), and the expression levels were

calculated by us. As mentioned above, quality control and filtering of raw reads were performed by FastQC and trimmomatic, respectively. We also used samtools (version: 1.15.1) to remove the ribosomal RNA-derived sequences in the *B. malayi (Danecek, et al. 2021)*. The filtered reads were mapped to the reference transcript models (*B. malayi*: PRJNA1072 and *A. ceylanicum*: PRJNA231479, WormBase Parasite (Howe, et al. 2017)) using RSEM/bowtie2 (version: v1.3.1, rsem-calculate-expression --paired-end --bowtie2) to calculate expression levels (TPM) (Li and Dewey 2011). Molting stages were referred from original/previous papers (Kim, et al. 2013; Cotton, et al. 2014; Leroux, et al. 2018; Bernot, et al. 2020; Grote, et al. 2020; Sun, et al. 2021; Shears and Grencis 2022). Expression levels of the transcripts corresponding to the *ecr* and *hr3,* which were identified in the above screenings, were obtained from each transcriptome dataset (the average of TPM was calculated in the case of having replicates at the same stage). In the transcriptome data of *G. pallida*, the gene model of *hr3* was inappropriately reconstructed into two models (id: GPLIN_000052400 and GPLIN_000052600). Thus, the expression levels were calculated by summing the expression levels of the two models at each time point.

Data curation

Sun et al., 2021 originally provided the 1–2 h interval transcriptome data of *P. pacifucs* from 0 to 58 h after hatching (i.e., 0, 1, 3, 5, ... 58 h) (Sun, et al. 2021). In our preliminary analysis, we found that the data contained an overall fluctuating expression pattern throughout the examined stages (Fig. S6A). Therefore, we divided the time points into overlapping windows of three time points each, and the mean was calculated for each window. For example, the first time-window was grouped by the data at 0, 1, and 3 h, and the mean value represents the data at 1 h. The second window included the data at 1, 3, and 5 h, and the mean value represents the data at 3 h. Using this method, we obtained the corrected expression profiles, which tends to remove the effects of fluctuating expression due to biological or technical differences on individual development (Fig. S6B).

Unbiased screening of NRs for identifying molting regulators

With reference to our previous work (Yamakawa and Hejnol 2024), the expression profiles (TPM matrices) of four nematode transcriptome data were classified into 5–7 clusters using fuzzy c-mean clustering (Fig. S7: *A. ceylanicum*, *G. pallida*, *B. malayi*, and *T. suis*). Analysis was carried out using R and its package e1071 (version: 1.7.11: https://cran.r-project.org/web/packages/e1071/index.html). From such clustering, the genes in the cluster(s) that showed a positively correlated expression pattern with molting cycles were extracted (Fig. S7, green shades, *A. ceylanicum*: 8110, *G. pallida*: 3383, *B. malayi*: 7114, and *T. suis*: 2896 genes). In addition, Sun et al. 2021 and Kim et al. 2013 extracted the genes whose expression showed an oscillatory pattern along the molting cycle in *P. pacificus* (2,964 genes) and *C. elegans* (1,592 genes: assigned to clusters 1–6 in Kim et al., 2013), respectively (Kim, et al. 2013; Sun, et al. 2021). As described above, OrthoFinder (Emms and Kelly 2019) was used to extract OGs among the screened genes, and this result

identified 5,180 OGs. Among 5,180 OGs, 55 OGs contain one or more genes from all species. We extracted 168 genes which were assigned into any 55 OGs in *C. elegans.* Finally, we searched for the presence of TF and NR domains in the represented the *C. elegans* 168 genes using Hmmer search (Johnson, et al. 2010) (see above).

6. Prediction of heterodimer strcuture

Foldseek search for the identification of the candidate proteins

First, we extracted the ligand-binding domain of USP from *Drosophila melanogaster* (UniProt: P20153) using the NCBI Conserved Domain Search tool (https://www.ncbi.nlm.nih.gov/Structure/cdd/wrpsb.cgi) (Blum, et al. 2024). We performed a Foldseek Search on the Foldseek web server (https://search.foldseek.com/search) and predicted the three-dimensional structure of USP with the 3Di/AA mode using sequence information (van Kempen, et al. 2024). We used this prediction as a query and targeted the AFDB-PROTEOME database in *C. elegans* (UP000001940). The results of this search are shown in Table S2. Subsequent analysis focused on five candidate proteins (NHR-64, NHR-69, NHR-35, NHR-49, and NHR-14). The orthologous genes were identified in several nematode species using BLAST and phylogenetic analyses (Enoplida: *Pontonema vulgare*, *Trissonchulus latispiculum*; Trichinellida: *Trichuris murris*; Dorylaimida: *Mesodorylaimus YZB24*; Spirurina: *Ascaris suum* and *Brugia malayi*; Tylenchina: *Globodera pallida*, *Steinernema monticolum*, and *Meloidogyne arenaria*; and Rhabditina: *Caenorhabditis elegans*, *Heligmosomoides polygyrus*, *Ancylostoma ceylanicum*, and, *Pristionchus pacificus*). The phylogenetic tree is available in the supplementary dataset, and Fig. S9 shows part of the tree (the USP and HNF4 clade).

Prediction of heterodimer interaction

The ColabFold interface was used to perform AlphaFold2 and AlphaFold2-Multimer analyses (Evans, et al. 2022; Mirdita, et al. 2022). The sequences used in the analysis were obtained from the above analysis or from UniProt (*D. melanogaster* ECR: P34021 and HNF4: P49866). The ligand binding domains were extracted using the NCBI Conserved Domain Search tool. The sequences were assigned to the ColabFold interface and analyzed with the default settings (e.g., num_relax = 0 and template_mode = none). Five protein structure models were predicted in each analysis. We presented the 3D model and ipTM score of the most reliable model in the main text (Figs. 6 and S11). The 3D models of the proteins were generated using PyMOL (version 3.1, https://www.pymol.org/), and the heat maps were obtained from the ColabFold output files. The original output files of this analysis are available in the supplementary dataset.

7. Data visualization

We used R (version: 4.3.3) (Team 2024) and its packages such as Tydyverse (version: 2.0.0) (Wickham, et al. 2019), ggtree (version: 3.10.1) (Xu, et al. 2022), ggstance (version: 0.3.7, https://github.com/lionel-/ggstance), ggvenn (version: 0.1.10, https://github.com/yanlinlin82/ggvenn), and ape (version: 5.8, https://cran.r-project.org/web/packages/ape/index.html) to analyze and visualize the results. Images for Fig. S5 are from PHYLOPIC (https://www.phylopic.org/).

Acknowledgments

We thank all current and former member of the Hejnol laboratory. In particular, we thank Nina Levin for proofreading of the manuscript. This study was supported by JSPS Oversea Fellowship (Japan Society for the Promotion of Science, to S.Y.), IMPULSE project (Friedrich Schiller University Jena, to S.Y.), Deutsche Forschungsgemeinschaft (project number 519107654, to A.H.), and the HFSP grant (RGP0041/2022, to A.H.).

Supplementary information

Supplementary dataset.

Supplementary figures (S1–S11)

Table S1. Annotation of the genes of 55 orthogroups in Caenorhabditis elegans

Table S2. Results of the Foldseek analysis

References

Adams S, Pathak P, Shao H, Lok JB, Pires-daSilva A. 2019. Liposome-based transfection enhances RNAi and CRISPR-mediated mutagenesis in non-model nematode systems. *Sci Rep.* **9**:483. 10.1038/s41598-018-37036-1

Aguinaldo AMA, Turbeville JM, Linford LS, Rivera MC, Garey JR, Raff RA, Lake JA. 1997. Evidence for a clade of nematodes, arthropods and other moulting animals. *Nature.* **387**:489-493.

Ahmed M, Roberts NG, Adediran F, Smythe AB, Kocot KM, Holovachov O. 2022. Phylogenomic Analysis of the Phylum Nematoda: Conflicts and Congruences With Morphology, 18S rRNA, and Mitogenomes. *Frontiers in Ecology and Evolution.* **9**. 10.3389/fevo.2021.769565

Álvarez-Ortega S, Brito JA, Subbotin SA. 2019. Multigene phylogeny of root-knot nematodes and molecular characterization of Meloidogyne nataliei Golden, Rose & Bird, 1981 (Nematoda: Tylenchida). *Scientific Reports.* **9**:11788. 10.1038/s41598-019-48195-0

Antebi A. 2015. Nuclear receptor signal transduction in C. elegans. *WormBook.* **1**.

Barker G. 1992. THE EFFECTS OF ECDYSTEROIDS ON REPRODUCTION AND DEVELOPMENT IN THE FILARIAL NEMATODES DIROFILARIA IMMITIS AND BRUGIA PAHANGI (NEMATODES).

Barker G, Rees H. 1990. Ecdysteroids in nematodes. *Parasitology Today.* **6**:384-387.

Barker GC, Chitwood DJ, Rees HH. 1990. Ecdysteroids in helminths and annelids. *Invertebrate Reproduction & Development.* **18**:1-11. 10.1080/07924259.1990.9672124

Barker GC, Mercer JG, Rees HH, Howells RE. 1991. The effect of ecdysteroids on the microfilarial production ofBrugia pahangi and the control of meiotic reinitiation in the oocytes ofDirofilaria immitis. *Parasitology Research.* **77**:65-71. 10.1007/BF00934388

Bernot JP, Rudy G, Erickson PT, Ratnappan R, Haile M, Rosa BA, Mitreva M, O'Halloran DM, Hawdon JM. 2020. Transcriptomic analysis of hookworm Ancylostoma ceylanicum life cycle stages reveals changes in G-protein coupled receptor diversity associated with the onset of parasitism. *International Journal for Parasitology.* **50**:603-610. https://doi.org/10.1016/j.ijpara.2020.05.003

Blum M, Andreeva A, Florentino Laise C, Chuguransky Sara R, Grego T, Hobbs E, Pinto Beatriz L, Orr A, Paysan-Lafosse T, Ponamareva I, et al. 2024. InterPro: the protein sequence classification resource in 2025. *Nucleic Acids Research.* **53**:D444-D456. 10.1093/nar/gkae1082

Bolger AM, Lohse M, Usadel B. 2014. Trimmomatic: a flexible trimmer for Illumina sequence data. *Bioinformatics.* **30**:2114-2120.

Bonneton F, Chaumot A, Laudet V. 2008. Annotation of Tribolium nuclear receptors reveals an increase in evolutionary rate of a network controlling the ecdysone cascade. *Insect Biochem Mol Biol.* **38**:416-429. 10.1016/j.ibmb.2007.10.006

Browning C, McEwen AG, Mori K, Yokoi T, Moras D, Nakagawa Y, Billas IML. 2021. Nonsteroidal ecdysone receptor agonists use a water channel for binding to the ecdysone receptor complex EcR/USP. *J Pestic Sci.* **46**:88-100. 10.1584/jpestics.D20-095

Cao M. 2023. CRISPR-Cas9 genome editing in Steinernema entomopathogenic nematodes. *bioRxiv.*2023.2011.2024.568619. 10.1101/2023.11.24.568619

Capella-Gutiérrez S, Silla-Martínez JM, Gabaldón T. 2009. trimAl: a tool for automated alignment trimming in large-scale phylogenetic analyses. *Bioinformatics.* **25**:1972-1973. 10.1093/bioinformatics/btp348

Cleator M, Delves CJ, Howells RE, Rees HH. 1987. Identity and tissue localization of free and conjugated ecdysteroids in adults of Dirofilaria immitis and Ascaris suum. *Molecular and Biochemical Parasitology.* **25**:93-105. https://doi.org/10.1016/0166-6851(87)90022-3

Cotton JA, Lilley CJ, Jones LM, Kikuchi T, Reid AJ, Thorpe P, Tsai IJ, Beasley H, Blok V, Cock PJA, et al. 2014. The genome and life-stage specific transcriptomes of Globodera pallidaelucidate key aspects of plant parasitism by a cyst nematode. *Genome Biology.* **15**:R43. 10.1186/gb-2014-15-3-r43

Cunha TJ, de Medeiros BAS, Lord A, Sørensen MV, Giribet G. 2023. Rampant loss of universal metazoan genes revealed by a chromosome-level genome assembly of the parasitic Nematomorpha. *Current Biology.* **33**:3514-3521.e3514. https://doi.org/10.1016/j.cub.2023.07.003

Danecek P, Bonfield JK, Liddle J, Marshall J, Ohan V, Pollard MO, Whitwham A, Keane T, McCarthy SA, Davies RM, et al. 2021. Twelve years of SAMtools and BCFtools. *Gigascience.* **10**. 10.1093/gigascience/giab008

Dayi M, Kanzaki N, Sun S, Ide T, Tanaka R, Masuya H, Okabe K, Kajimura H, Kikuchi T. 2021. Additional description and genome analyses of Caenorhabditis auriculariae representing the basal lineage of genus Caenorhabditis. *Scientific Reports.* **11**:6720. 10.1038/s41598-021-85967-z

Delves CJ, Howells RE, Post RJ. 1986. Gametogenesis and fertilization in Dirofilaria immitis (Nematoda: Filarioidea). *Parasitology.* **92**:181-197. 10.1017/S003118200006354X

Dennis RD. 1976. Insect morphogenetic hormones and developmental mechanisms in the nematode, Nematospiroides dubius. *Comparative Biochemistry and Physiology Part A: Physiology.* **53**:53-56. https://doi.org/10.1016/S0300-9629(76)80009-6

Dumidae A, Luangsawang K, Thanwisai A, Vitta A. 2023. Identification and genetic characterization of Angiostrongylus cantonensis isolated from the human eye. *Parasitology Research.* **122**:2217-2225. 10.1007/s00436-023-07922-3

Dunn CW, Hejnol A, Matus DQ, Pang K, Browne WE, Smith SA, Seaver E, Rouse GW, Obst M, Edgecombe GD. 2008. Broad phylogenomic sampling improves resolution of the animal tree of life. *Nature.* **452**:745-749.

Eleftheriadi K, Guiglielmoni N, Salces-Ortiz J, Vargas-Chavez C, Martínez-Redondo GI, Gut M, Flot J-F, Schmidt-Rhaesa A, Fernández R. (10_24072_pcjournal_381 co-authors). 2024. The genome sequence of the Montseny horsehair worm, Gordionus montsenyensis sp. nov., a key resource to investigate Ecdysozoa evolution. *Peer Community Journal.* **4**. 10.24072/pcjournal.381

Emms DM, Kelly S. 2019. OrthoFinder: phylogenetic orthology inference for comparative genomics. *Genome Biology.* **20**:1-14.

Evans R, O'Neill M, Pritzel A, Antropova N, Senior A, Green T, Žídek A, Bates R, Blackwell S, Yim J, et al. 2022. Protein complex prediction with AlphaFold-Multimer. *bioRxiv.*2021.2010.2004.463034. 10.1101/2021.10.04.463034

Evershed RP, Mercer JG, Rees HH. 1987. Capillary gas chromatography-mass spectrometry of ecdysteroids. *Journal of Chromatography A.* **390**:357-369. https://doi.org/10.1016/S0021-9673(01)94387-0

Fasteen TD, Hernandez MR, Policastro RA, Sterrett MC, Zenter GE, Tennessen JM. 2025. The Drosophila estrogen-related receptor promotes triglyceride storage within the larval fat body. *J Lipid Res.* **66**:100815. 10.1016/j.jlr.2025.100815

Fleming MW. 1985. Ascaris suum: role of ecdysteroids in molting. *Exp Parasitol.* **60**:207-210. 10.1016/0014-4894(85)90024-4

Frand AR, Russel S, Ruvkun G. 2005. Functional Genomic Analysis of C. elegans Molting. *PLOS Biology.* **3**:e312. 10.1371/journal.pbio.0030312

885 Gao Y, Zhang X, Wei J, Sun X, Yuan J, Li F, Xiang J. 2015. Whole Transcriptome Analysis
886 Provides Insights into Molecular Mechanisms for Molting in Litopenaeus vannamei. *PLoS One.*
887 **10**:e0144350. 10.1371/journal.pone.0144350

888 Giribet G, Edgecombe GD. 2017. Current Understanding of Ecdysozoa and its Internal
889 Phylogenetic Relationships. *Integrative and Comparative Biology.* **57**:455-466.
890 10.1093/icb/icx072

891 Gissendanner CR, Crossgrove K, Kraus KA, Maina CV, Sluder AE. 2004. Expression and function
892 of conserved nuclear receptor genes in Caenorhabditis elegans. *Developmental Biology.* **266**:399-
893 416. https://doi.org/10.1016/j.ydbio.2003.10.014

894 Gonzalez Akimori D, Dalessandro EJ, Nolan TJ, Stieha CR, Lok JB, Stoltzfus JDC. 2021.
895 Transcriptional profiles in Strongyloides stercoralis males reveal deviations from the
896 Caenorhabditis sex determination model. *Scientific Reports.* **11**:8254. 10.1038/s41598-021-87478-
897 3

898 Graham LD, Kotze AC, Fernley RT, Hill RJ. 2010. An ortholog of the ecdysone receptor protein
899 (EcR) from the parasitic nematode Haemonchus contortus. *Molecular and Biochemical*
900 *Parasitology.* **171**:104-107. https://doi.org/10.1016/j.molbiopara.2010.03.003

901 Grote A, Li Y, Liu C, Voronin D, Geber A, Lustigman S, Unnasch TR, Welch L, Ghedin E. 2020.
902 Prediction pipeline for discovery of regulatory motifs associated with Brugia malayi molting. *PLOS*
903 *Neglected Tropical Diseases.* **14**:e0008275. 10.1371/journal.pntd.0008275

904 Hada K, Asahina M, Hasegawa H, Kanaho Y, Slack FJ, Niwa R. 2010. The nuclear receptor gene
905 nhr-25 plays multiple roles in the Caenorhabditis elegans heterochronic gene network to control
906 the larva-to-adult transition. *Developmental Biology.* **344**:1100-1109.

907 Hayes GD, Frand AR, Ruvkun G. 2006. The mir-84 and let-7 paralogous microRNA genes of
908 Caenorhabditis elegans direct the cessation of molting via the conserved nuclear hormone receptors
909 NHR-23 and NHR-25. *Development.* **133**:4631-4641. 10.1242/dev.02655

910 Hejnol A, Obst M, Stamatakis A, Ott M, Rouse GW, Edgecombe GD, Martinez P, Baguñà J, Bailly
911 X, Jondelius U. 2009. Assessing the root of bilaterian animals with scalable phylogenomic
912 methods. *Proceedings of the Royal Society B: Biological Sciences.* **276**:4261-4270.

913 Hellekes V, Claus D, Seiler J, Illner F, Schiffer PH, Kroiher M. 2023. CRISPR/Cas9 mediated gene
914 editing in non-model nematode Panagrolaimus sp. PS1159. *Front Genome Ed.* **5**:1078359.
915 10.3389/fgeed.2023.1078359

916 Hendriks GJ, Gaidatzis D, Aeschimann F, Großhans H. 2014. Extensive oscillatory gene expression
917 during C. elegans larval development. *Mol Cell.* **53**:380-392. 10.1016/j.molcel.2013.12.013

918 Henschel R, Lieber M, Wu L-S, Nista PM, Haas BJ, LeDuc RD editors. Proceedings of the 1st
919 Conference of the Extreme Science and Engineering Discovery Environment: Bridging from the
920 eXtreme to the campus and beyond. 2012.

921 Herranz M, Stiller J, Worsaae K, Sørensen MV. 2022. Phylogenomic analyses of mud dragons
922 (Kinorhyncha). *Molecular Phylogenetics and Evolution.* **168**:107375.
923 https://doi.org/10.1016/j.ympev.2021.107375

924 Hill RJ, Billas IM, Bonneton F, Graham LD, Lawrence MC. 2013. Ecdysone receptors: from the
925 Ashburner model to structural biology. *Annu Rev Entomol.* **58**:251-271. 10.1146/annurev-ento-
926 120811-153610

927 Hiroki S, Yoshitane H. 2024. Ror homolog nhr-23 is essential for both developmental clock and
928 circadian clock in C. elegans. *Communications Biology.* **7**:243. 10.1038/s42003-024-05894-3

929 Hitcho PJ, Thorson RE. 1971. Possible molting and maturation controls in Trichinella spiralis. *The*
930 *Journal of Parasitology.*787-793.

Howe KL, Bolt BJ, Shafie M, Kersey P, Berriman M. 2017. WormBase ParaSite − a comprehensive resource for helminth genomics. *Molecular and Biochemical Parasitology.* **215**:2-10. https://doi.org/10.1016/j.molbiopara.2016.11.005

Hu L, Zhang M, Sun Y, Bu Y. 2020. Characterization and phylogenetic analysis of the first complete mitochondrial genome of Cylicocyclus radiatus. *Veterinary Parasitology.* **281**:109097. https://doi.org/10.1016/j.vetpar.2020.109097

Hyde CJ, Elizur A, Ventura T. 2019. The crustacean ecdysone cassette: A gatekeeper for molt and metamorphosis. *The Journal of Steroid Biochemistry and Molecular Biology.* **185**:172-183.

Johnson LC, Vo AA, Clancy JC, Myles KM, Pooranachithra M, Aguilera J, Levenson MT, Wohlenberg C, Rechtsteiner A, Ragle JM, et al. 2023. NHR-23 activity is necessary for C. elegans developmental progression and apical extracellular matrix structure and function. *Development.* **150**. 10.1242/dev.201085

Johnson LS, Eddy SR, Portugaly E. 2010. Hidden Markov model speed heuristic and iterative HMM search procedure. *BMC bioinformatics.* **11**:1-8.

Jumper J, Evans R, Pritzel A, Green T, Figurnov M, Ronneberger O, Tunyasuvunakool K, Bates R, Žídek A, Potapenko A, et al. 2021. Highly accurate protein structure prediction with AlphaFold. *Nature.* **596**:583-589. 10.1038/s41586-021-03819-2

Katoh K, Standley DM. 2013. MAFFT multiple sequence alignment software version 7: improvements in performance and usability. *Mol Biol Evol.* **30**:772-780. 10.1093/molbev/mst010

Kim D, Grün D, van Oudenaarden A. 2013. Dampening of expression oscillations by synchronous regulation of a microRNA and its target. *Nat Genet.* **45**:1337-1344. 10.1038/ng.2763

Kinney B, Sahu S, Stec N, Hills-Muckey K, Adams DW, Wang J, Jaremko M, Joshua-Tor L, Keil W, Hammell CM. 2023. A circadian-like gene network programs the timing and dosage of heterochronic miRNA transcription during C. elegans development. *Dev Cell.* **58**:2563-2579.e2568. 10.1016/j.devcel.2023.08.006

Kostrouchova M, Kostrouch Z. 2015. Nuclear receptors in nematode development: Natural experiments made by a phylum. *Biochimica et Biophysica Acta (BBA) - Gene Regulatory Mechanisms.* **1849**:224-237. https://doi.org/10.1016/j.bbagrm.2014.06.016

Kostrouchova M, Krause M, Kostrouch Z, Rall JE. 1998. CHR3: a Caenorhabditis elegans orphan nuclear hormone receptor required for proper epidermal development and molting. *Development.* **125**:1617-1626. 10.1242/dev.125.9.1617

Kostrouchova M, Krause M, Kostrouch Z, Rall JE. 2001. Nuclear hormone receptor CHR3 is a critical regulator of all four larval molts of the nematode Caenorhabditis elegans. *Proc Natl Acad Sci U S A.* **98**:7360-7365. 10.1073/pnas.131171898

Kouns NA, Nakielna J, Behensky F, Krause MW, Kostrouch Z, Kostrouchova M. 2011. NHR-23 dependent collagen and hedgehog-related genes required for molting. *Biochem Biophys Res Commun.* **413**:515-520. 10.1016/j.bbrc.2011.08.124

Kozlova T, Thummel CS. 2000. Steroid Regulation of Postembryonic Development and Reproduction in Drosophila. *Trends in Endocrinology & Metabolism.* **11**:276-280. https://doi.org/10.1016/S1043-2760(00)00282-4

Lachaise F, Le Roux A, Hubert M, Lafont R. 1993. The molting gland of crustaceans: localization, activity, and endocrine control (a review). *Journal of Crustacean Biology.* **13**:198-234.

Lai C-K, Lee Y-C, Ke H-M, Lu MR, Liu W-A, Lee H-H, Liu Y-C, Yoshiga T, Kikuchi T, Chen PJ, et al. 2022. The Aphelenchoides genomes reveal substantial horizontal gene transfers in the last common ancestor of free-living and major plant parasitic nematodes. *bioRxiv.*2022.2009.2013.507733. 10.1101/2022.09.13.507733

977 Leroux LP, Nasr M, Valanparambil R, Tam M, Rosa BA, Siciliani E, Hill DE, Zarlenga DS,
978 Jaramillo M, Weinstock JV, et al. 2018. Analysis of the Trichuris suis excretory/secretory proteins
979 as a function of life cycle stage and their immunomodulatory properties. *Sci Rep.* **8**:15921.
980 10.1038/s41598-018-34174-4

981 Li B, Dewey CN. 2011. RSEM: accurate transcript quantification from RNA-Seq data with or
982 without a reference genome. *BMC bioinformatics.* **12**:1-16.

983 Liang B, Ferguson K, Kadyk L, Watts JL. 2010. The role of nuclear receptor NHR-64 in fat storage
984 regulation in Caenorhabditis elegans. *PLoS One.* **5**:e9869. 10.1371/journal.pone.0009869

985 Lindblom TH, Dodd AK. 2006. Xenobiotic detoxification in the nematode Caenorhabditis elegans.
986 *J Exp Zool A Comp Exp Biol.* **305**:720-730. 10.1002/jez.a.324

987 Lindblom TH, Pierce GJ, Sluder AE. 2001. A C. elegans orphan nuclear receptor contributes to
988 xenobiotic resistance. *Curr Biol.* **11**:864-868. 10.1016/s0960-9822(01)00236-6

989 Liu L, Liu X, Fu Y, Fang W, Wang C. 2022. Whole-body transcriptome analysis provides insights
990 into the cascade of sequential expression events involved in growth, immunity, and metabolism
991 during the molting cycle in Scylla paramamosain. *Scientific Reports.* **12**:11395. 10.1038/s41598-
992 022-14783-w

993 Malakhov U. 1986. Nematodes: Structure, development, classification and phylogeny.

994 McCann K, Grant W, Doyle S. 2021. The genome sequence of the Australian filarial nematode,
995 Cercopithifilaria johnstoni [version 2; peer review: 3 approved]. *Wellcome Open Research.* **6**.
996 10.12688/wellcomeopenres.17258.2

997 Meeuse MW, Hauser YP, Morales Moya LJ, Hendriks GJ, Eglinger J, Bogaarts G, Tsiairis C,
998 Großhans H. 2020. Developmental function and state transitions of a gene expression oscillator in
999 Caenorhabditis elegans. *Mol Syst Biol.* **16**:e9498. 10.15252/msb.20209498

1000 Meeuse MWM, Hauser YP, Nahar S, Smith AAT, Braun K, Azzi C, Rempfler M, Großhans H.
1001 2023. C. elegans molting requires rhythmic accumulation of the Grainyhead/LSF transcription
1002 factor GRH-1. *Embo j.* **42**:e111895. 10.15252/embj.2022111895

1003 Mirdita M, Schütze K, Moriwaki Y, Heo L, Ovchinnikov S, Steinegger M. 2022. ColabFold:
1004 making protein folding accessible to all. *Nature Methods.* **19**:679-682. 10.1038/s41592-022-01488-
1005 1

1006 Monsalve GC, Van Buskirk C, Frand AR. 2011. LIN-42/PERIOD controls cyclical and
1007 developmental progression of C. elegans molts. *Curr Biol.* **21**:2033-2045.
1008 10.1016/j.cub.2011.10.054

1009 Murai Y, Yagi-Utsumi M, Fujiwara M, Tanaka S, Tomita M, Kato K, Arakawa K. 2021.
1010 Multiomics study of a heterotardigrade, Echinisicus testudo, suggests the possibility of convergent
1011 evolution of abundant heat-soluble proteins in Tardigrada. *BMC Genomics.* **22**:813.
1012 10.1186/s12864-021-08131-x

1013 Nielsen C. 2012. Animal evolution: interrelationships of the living phyla: Oxford University Press.

1014 Niwa R, Niwa YS. 2014. Enzymes for ecdysteroid biosynthesis: their biological functions in insects
1015 and beyond. *Bioscience, biotechnology, and biochemistry.* **78**:1283-1292.

1016 Öztürk-Çolak A, Marygold SJ, Antonazzo G, Attrill H, Goutte-Gattat D, Jenkins VK, Matthews
1017 BB, Millburn G, dos Santos G, Tabone CJ, et al. 2024. FlyBase: updates to the Drosophila genes
1018 and genomes database. *Genetics.* **227**. 10.1093/genetics/iyad211

1019 Parihar M, Minton RL, Flowers S, Holloway A, Morehead BE, Paille J, Gissendanner CR. 2010.
1020 The genome of the nematode Pristionchus pacificus encodes putative homologs of RXR/Usp and

1021 EcR. *General and Comparative Endocrinology.* **167**:11-17.
1022 https://doi.org/10.1016/j.ygcen.2010.02.005

1023 Park D, Jones KL, Lee H, Snutch TP, Taubert S, Riddle DL. 2012. Repression of a potassium
1024 channel by nuclear hormone receptor and TGF-β signaling modulates insulin signaling in
1025 Caenorhabditis elegans. *PLoS Genet.* **8**:e1002519. 10.1371/journal.pgen.1002519

1026 Patel R, Galagali H, Kim JK, Frand AR. 2022. Feedback between a retinoid-related nuclear receptor
1027 and the let-7 microRNAs controls the pace and number of molting cycles in C. elegans. *Elife.* **11**.
1028 10.7554/eLife.80010

1029 Pathare PP, Lin A, Bornfeldt KE, Taubert S, Van Gilst MR. 2012. Coordinate Regulation of Lipid
1030 Metabolism by Novel Nuclear Receptor Partnerships. *PLOS Genetics.* **8**:e1002645.
1031 10.1371/journal.pgen.1002645

1032 Patil G, van Zon JS. 2024. Timers, variability, and body-wide coordination: C. elegans as a model
1033 system for whole-animal developmental timing. *Curr Opin Genet Dev.* **85**:102172.
1034 10.1016/j.gde.2024.102172

1035 Patke A, Young MW, Axelrod S. 2020. Molecular mechanisms and physiological importance of
1036 circadian rhythms. *Nature reviews Molecular cell biology.* **21**:67-84.

1037 Pérez E, Bourguet W, Gronemeyer H, de Lera AR. 2012. Modulation of RXR function through
1038 ligand design. *Biochimica et Biophysica Acta (BBA) - Molecular and Cell Biology of Lipids.*
1039 **1821**:57-69. https://doi.org/10.1016/j.bbalip.2011.04.003

1040 Qing X, Zhang YM, Sun S, Ahmed M, Lo W-S, Bert W, Holovachov O, Li H. 2024. Phylogenomic
1041 Insights into the Evolution and Origin of Nematoda. *Systematic Biology.* **74**:349-358.
1042 10.1093/sysbio/syae073

1043 Schumann I, Kenny N, Hui J, Hering L, Mayer G. 2018. Halloween genes in panarthropods and
1044 the evolution of the early moulting pathway in Ecdysozoa. *R Soc Open Sci.* **5**:180888.
1045 10.1098/rsos.180888

1046 Schwarz EM, Baniya A, Heppert JK, Schwartz HT, Tan C-H, Antoshechkin I, Sternberg PW,
1047 Goodrich-Blair H, Dillman AR. 2025. Genomes of the entomopathogenic nematode
1048 Steinernema hermaphroditum and its associated bacteria.
1049 *bioRxiv.*2025.2001.2009.632278. 10.1101/2025.01.09.632278

1050 Shang Kuan T-C, Prichard RK. 2020. Developmental regulation of Dirofilaria immitis
1051 microfilariae and evaluation of ecdysone signaling pathway transcript level using droplet digital
1052 PCR. *Parasites & Vectors.* **13**:614. 10.1186/s13071-020-04480-w

1053 Shea C, Hough D, Xiao J, Tzertzinis G, Maina CV. 2004. An rxr/usp homolog from the parasitic
1054 nematode, Dirofilaria immitis. *Gene.* **324**:171-182.

1055 Shea C, Richer J, Tzertzinis G, Maina CV. 2010. An EcR homolog from the filarial parasite,
1056 Dirofilaria immitis requires a ligand-activated partner for transactivation. *Molecular and*
1057 *Biochemical Parasitology.* **171**:55-63.

1058 Shears RK, Grencis RK. 2022. Whipworm secretions and their roles in host-parasite interactions.
1059 *Parasites & Vectors.* **15**:348. 10.1186/s13071-022-05483-5

1060 Smythe AB, Holovachov O, Kocot KM. 2019. Improved phylogenomic sampling of free-living
1061 nematodes enhances resolution of higher-level nematode phylogeny. *BMC Evolutionary Biology.*
1062 **19**:121. 10.1186/s12862-019-1444-x

1063 Spangler RK, Braun K, Ashley GE, van der Does M, Wruck D, Coronado AR, Matthew Ragle J,
1064 Iesmantavicius V, Morales Moya LJ, Jonnalagadda K, et al. 2024. A conserved chronobiological
1065 complex times C. elegans development. *bioRxiv.* 10.1101/2024.05.09.593322

1066 Stamatakis A. 2014. RAxML version 8: a tool for phylogenetic analysis and post-analysis of large
1067 phylogenies. *Bioinformatics.* **30**:1312-1313.

1068 Subramoniam T. 2000. Crustacean ecdysteriods in reproduction and embryogenesis. *Comparative*
1069 *Biochemistry and Physiology Part C: Pharmacology, Toxicology and Endocrinology.* **125**:135-
1070 156. https://doi.org/10.1016/S0742-8413(99)00098-5

1071 Sun S, Rödelsperger C, Sommer RJ. 2021. Single worm transcriptomics identifies a developmental
1072 core network of oscillating genes with deep conservation across nematodes. *Genome Res.* **31**:1590-
1073 1601. 10.1101/gr.275303.121

1074 Sural S, Hobert O. 2021. Nematode nuclear receptors as integrators of sensory information. *Current*
1075 *Biology.* **31**:4361-4366.e4362. 10.1016/j.cub.2021.07.019

1076 Taubenheim J, Kortmann C, Fraune S. 2021. Function and Evolution of Nuclear Receptors in
1077 Environmental-Dependent Postembryonic Development. *Frontiers in Cell and Developmental*
1078 *Biology.* **9**. 10.3389/fcell.2021.653792

1079 Taubert S, Ward JD, Yamamoto KR. 2011. Nuclear hormone receptors in nematodes: evolution
1080 and function. *Mol Cell Endocrinol.* **334**:49-55. 10.1016/j.mce.2010.04.021

1081 Team RC. 2024. R: A language and environment for statistical computing. R Foundation for
1082 Statistical Computing, Vienna, Austria.

1083 Thummel CS. 1996. Flies on steroids — Drosophila metamorphosis and the mechanisms of steroid
1084 hormone action. *Trends in Genetics.* **12**:306-310. https://doi.org/10.1016/0168-9525(96)10032-9

1085 Tsiairis C, Großhans H. 2021. Gene expression oscillations in C. elegans underlie a new
1086 developmental clock. *Curr Top Dev Biol.* **144**:19-43. 10.1016/bs.ctdb.2020.11.001

1087 Tzertzinis G, Egaña AL, Palli SR, Robinson-Rechavi M, Gissendanner CR, Liu C, Unnasch TR,
1088 Maina CV. 2010. Molecular Evidence for a Functional Ecdysone Signaling System in Brugia
1089 malayi. *PLOS Neglected Tropical Diseases.* **4**:e625. 10.1371/journal.pntd.0000625

1090 van Kempen M, Kim SS, Tumescheit C, Mirdita M, Lee J, Gilchrist CLM, Söding J, Steinegger
1091 M. 2024. Fast and accurate protein structure search with Foldseek. *Nature Biotechnology.* **42**:243-
1092 246. 10.1038/s41587-023-01773-0

1093 Vogeler S, Galloway TS, Lyons BP, Bean TP. 2014. The nuclear receptor gene family in the Pacific
1094 oyster, Crassostrea gigas, contains a novel subfamily group. *BMC Genomics.* **15**:369.
1095 10.1186/1471-2164-15-369

1096 Wickham H, Averick M, Bryan J, Chang W, McGowan LDA, François R, Grolemund G, Hayes
1097 A, Henry L, Hester J. 2019. Welcome to the Tidyverse. *Journal of open source software.* **4**:1686.

1098 Xu S, Li L, Luo X, Chen M, Tang W, Zhan L, Dai Z, Lam TT, Guan Y, Yu G. 2022. Ggtree: A
1099 serialized data object for visualization of a phylogenetic tree and annotation data. *iMeta.* **1**:e56.
1100 https://doi.org/10.1002/imt2.56

1101 Yamakawa S, Hejnol A. 2024. Ecdysteroid-dependent molting in tardigrades. *Current Biology.*
1102 **34**:p5804-5812.e5804. 10.1016/j.cub.2024.10.054

1103 Yamakawa S, Yamazaki A, Morino Y, Wada H. 2023. Early expression onset of tissue-specific
1104 effector genes during the specification process in sea urchin embryos. *EvoDevo.* **14**:7.
1105 10.1186/s13227-023-00210-2

1106 Yamanaka N, Rewitz KF, O'Connor MB. 2013. Ecdysone control of developmental transitions:
1107 lessons from Drosophila research. *Annual review of entomology.* **58**:497-516.

1108